FOURTH EUROPEAN ROTORCRAFT AND POWERED LIFT AIRCRAFT FORUM

Paper No. 28

GUST RESPONSE AND ITS ALLEVIATION FOR A HINGELESS HELICOPTER ROTOR IN CRUISING FLIGHT

Masahiro Yasue
Charles A. Vehlow
Norman D. Ham

September 13 - 15, 1978
STRESA - ITALY

Associazione Italiana di Aeronautica ed Astronautica
Associazione Industrie Aerospaziali

GUST RESPONSE AND ITS ALLEVIATION FOR A HINGELESS HELICOPTER ROTOR IN CRUISING FLIGHT*

by

Masahiro Yasue
Charles A. Vehlow
Norman D. Ham

Department of Aeronautics and Astronautics
Massachusetts Institute of Technology

ABSTRACT

The vertical gust response and its alleviation for hingeless helicopter rotor blades in cruising flight is studied theoretically and experimentally. An evaluation is performed of the effectiveness of torsional stiffness variation in conjunction with chordwise center-of-gravity shift in alleviating the blade flapping response to decrease the root bending moment.

The theoretical analysis utilizes the equations of motion of hingeless rotor blades exposed to vertical gusts in forward flight for the flapping, lagging, and elastic and rigid pitch degrees of freedom. The equations include the effect of steady-state deflections in the trim conditions and various hingeless rotor configurations such as precone, droop and torque offset as well as chordwise center-of-gravity shift and aerodynamic center offset.

The experimental program involves the wind tunnel tests of a five-foot diameter rotor subject to a sinusoidal waveform gust. Testing involves variation of the blade chordwise center-of-gravity location, the blade torsional stiffness, rotor advance ratio, and vertical gust frequency.

* This research was sponsored by the Naval Air Systems Command, United States Navy.

1. Introduction

Over the last decade the hingeless rotor has attained acceptance as an attractive concept for rotorcraft, and considerable research, development, and testing has been conducted. The main advantages of this system are improved flying qualities, and design simplicity of the rotor and rotor hub. However, rotor blade aeroelastic stability and response become more sensitive because of structural coupling between bending (flapwise and chordwise) and torsion of the slender cantilever blade. Also, hingeless-rotor helicopters are sensitive to atmospheric turbulence. Therefore, the study of the response of the hingeless rotor to atmospheric turbulence is necessary in evaluating the blade fatigue characteristics and the riding comfort of the vehicle, and in the development of gust alleviation systems.

Unfortunately, very little literature is available on the response of the helicopter to atmospheric turbulence. References 1, 2, 3, and 4 analyzed the blade response to random inputs, using various methods of computing the random response of a time-varying linear system.

Arcidiacono et al. (Ref. 5) conducted an analytical study of articulated helicopter response to various gust profiles such as sine-squared and ramp gusts. They confirmed that the current gust alleviation factors specified in MIL-S-8698(ARG) are too conservative. Judd and Newman (Ref. 6) analyzed the rotor and vehicle response to gusts and turbulence. The rotor response to step, ramp, and sinusoidal gusts was studied.

For the tilt-rotor aircraft, extensive analyses of the gust response in cruising flight were conducted by Johnson (Ref. 7) and Yasue (Ref. 8). In Ref. 7, Johnson summarized the comparison of theory with the results of full-scale tests of two proprotors in terms of critical damping ratios and frequencies of modes. The agreement between theory and experiment was good. He extended his theory (Ref. 9) to include various rotor parameters such as precone and droop as well as the transition flight regime between hovering and cruising flight. Concurrently with the extension of the theory, Frick and Johnson (Ref. 10) applied modern control theory to develop a gust alleviation system for the tilt-rotor. Wind tunnel experiments were conducted at M.I.T., using a one-ninth-scale tilt-rotor model subjected to vertical and longitudinal sinusoidal gusts as well as collective and cyclic pitch control inputs (Ref. 11). The experimental results showed good agreement with the theoretical analysis of Ref. 8. Further investigations were performed to develop a gust alleviation device for the gimballed tilt-rotor (Ref. 12), and subsequently, wind tunnel testing was conducted to verify the theoretical predictions (Ref. 13).

Finally, the effect of varying the blade chordwise is briefly reviewed. Miller (Ref. 14) suggested chordwise blade mass balance to improve helicopter flying qualities. Hirsh et al. (Ref. 15) applied chordwise mass balance to the articulated rotor helicopter XH-17 and reduced the vibration stresses by 35 to 45 percent. Miller and Ellis (Ref. 16) analyzed the effectiveness of chordwise mass balance to reduce the vibratory root shear of the articulated

helicopter. Reichert, Huber, and Oelker, Refs. 17 and 18, showed that a 2.5% forward shift of the center-of-gravity of the BO-105 blade reduced the rotor angle-of-attack instability. In conjunction with the improvement of the stability characteristics, a favorable gust response reduction was also obtained, as shown in Refs. 18 and 19. A 5% center-of-gravity forward shift reduced the flapping response by about 40% in trimmed flight at 100 knots, compared with no chordwise mass balance. Thus, blade center-of-gravity forward of the aerodynamic center will reduce both the angle-of-attack instability and the gust sensitivity.

The purpose of the present work is to validate the theory of Ref. 20 and to investigate the effectiveness of chordwise center-of-gravity shift in conjunction with blade torsional stiffness variation in alleviating the blade flapping response of the hingeless rotor blade theoretically and experimentally.

As the first step of the theoretical analysis, presented in Ref. 20, free vibration equations for the flap-lag-torsion-rigid pitch motion of the rotating nonuniform beam were developed including precone, droop, torque offset, offsets between the elastic axis and cross-sectional center of gravity, built-in twist, and collective pitch. The rigid-pitch motion is due to control linkage flexibility. Based on these equations, the natural frequencies and corresponding normal coupled mode shapes of a rotating nonuniform rotor blade were obtained using the finite-element method. By the use of Galerkin's Method, the equations of motion for the blade with aerodynamic forces were converted to modal equations. The equations included the effect of steady-state deflections and the quasi-steady assumption was employed for the aerodynamic forces. The coefficients of the equations are periodic in time in forward flight, so the harmonic balance approximation method (Ref. 21) was used to avoid the complexity of periodic coefficients. These modal equations with constant coefficients were used in the present study of the hingeless rotor response to a vertical gust in cruising flight.

The experimental program involved the design, construction, and testing of a five-foot diameter rotor. The rotor design was such that the torsional stiffness of the blade as well as the blade chordwise center-of-gravity location could be varied during the various phases of the test. The rotor was exposed to a sinusoidal waveform vertical gust and the flap, lag and torsion motion of the blade was measured.

2. Experimental Program

An overall view of the model rotor and mount is given in Fig. 1. The model rotor consists of three blades with an offset flapping hinge at 0.176R spanwise location. This flapping hinge configuration was adopted to obtain the desired flap, lag and torsion natural frequencies with the flexure system explained in detail later. The rotor diameter is approximately 5 feet and the blade chord is 2 inches. The blades have 8 degree linear geometrical twist and an NACA 0012 airfoil section. The model rotor is an approximate Froude-scaled dynamic model of a typical soft-inplane hingeless rotor. The model rotor solidity is 0.0704, which is roughly equal to the solidity of most

existing full-scale rotors in operation today. However, the Lock number is 2.27, which is very low in comparison with full size rotors. Additionally, because of the orientation of the gust generator the rotor disc is located vertically in order to use the lateral gust as the vertical gust in the helicopter sense. Blade characteristics used in the experiment are listed in Table 1.

To achieve the desired rotating natural frequencies of the blade lag and torsional motions, a flexure is placed between the blade and hub as shown in Figure 2. The chordwise bending and torsional stiffness of the flexure determines the rotating lag and torsional natural frequencies and the spanwise location of the hinge gives the appropriate flapping frequency. The cross-sectional dimensions (width and height) of the flexure, which was made of 17-7 PH stainless steel, were chosen to obtain the desired stiffness. In order to evaluate the rotating blade natural frequencies from the given stiffness of the flexure and blade, the computer program based on the analysis of Ref. 20 was used.

The physical properties of the model rotor such as mass distribution and stiffness were measured and are shown in Table 1.

Lead-lag dampers are used to overcome the lag resonance encountered in the preliminary experimental stage. The gravity force excited severe one-per-revolution lag motion when the rotor rotational speed was at the lag natural frequency since the rotor was mounted vertically, and the structural and aerodynamic lag damping of the blade was very small. The lag structural damping was 0.2% of critical without the lead-lag damper, and with the damper it increased to 7.0% of critical.

The rotor blade is rigidly attached to the rigid rotor hub with no pre-cone or droop. The blade collective pitch can be changed at the hub location; no cyclic pitch control is incorporated.

The rotor hub is rigidly mounted to the rotor shaft which runs across the tunnel horizontally as shown in Fig. 1. The rotor disc was located vertically to obtain the vertical gust effect from the existing gust generator at the M.I.T. Wright Brothers Wind Tunnel. The rotor shaft is mounted 3.5 feet above the tunnel floor to place the rotor in the center of the 7 x 10 foot elliptic cross-section of the wind tunnel. The rotor shaft is supported by two trunnions which are connected to the wind tunnel balance system. Rotor shaft tilting is also possible to simulate the helicopter forward flight cruising configuration. The shaft can be tilted up to 30 degrees forward.

The rotor is driven by a hydraulic motor mounted outside the tunnel and a flow control valve in the hydraulic system is used to vary the rotational speed between zero and approximately 1200 rpm.

Each blade flexure was instrumented with strain gages in order to detect lag and torsion motion. The lag bending strain gage was located at

0.128R spanwise station (1.1 inch from the cantilevered flexure root which is 2.4 inches long) and the torsion gage was at 0.15R spanwise location (1.7 inches from the cantilevered flexure root).

In order to detect the flapping motion a small .007-inch-thick leaf spring was placed between the blade and the flapping pin at the hinge location. The flapping hinge pin, fixed to the flexure, is extended slightly and slotted to provide a built-in mount for the root end of the cantilevered leaf spring. The outboard end of the leaf spring has a sliding fit in a blade-mounted fitting. The leaf spring provides negligible elastic restraint to the blade flapping motion. This leaf spring was also instrumented with strain gages for the measuring of blade flapping motion in terms of leaf spring bending strain. The instrumentation for flap, lag and torsion motion can be seen in Fig. 2.

In addition to the blade deflection signals, the rotor RPM and blade azimuth angle signal are available from one of the slip rings. Once per revolution the circuit on the slip ring is closed and provides the signal for the RPM frequency counter, while in the recorded time history the location where the circuit is closed gives the blade azimuth angle. The gust magnitude was measured using a hot wire placed at the rotor hub location and the gust frequency was measured on the gust generator.

The purpose of the wind tunnel tests was to validate the theory developed in Reference 20 and to investigate the reduction of blade bending motion due to a vertical gust utilizing blade chordwise mass unbalance as a passive control measure. One means of accomplishing the testing of the blades with different center-of-gravity locations would be to design and build rotor blades which actually had different center-of-gravity locations. This method, however, would have proved too costly and time consuming. Therefore, it was decided that through the addition of a variable weight placed at the blade tip, the designed center-of-gravity shift would be accomplished.

The scheme used to apply the tip weight to the model blade is shown in Fig. 3. A stainless steel sleeve/tube is attached to the blade tip. A tungsten slug, weighing 40 grams, is slipped inside the tube. By securing the slug at any location in the tube, an appropriate shift of the chordwise center-of-gravity either fore and aft was achieved.

The slug location allows for effective chordwise C.G. variation (C.G. location averaged in the spanwise direction) ranging from 35% chord from the leading edge (most aft position) to 18% chord (most forward position).

In order that no more than one blade of the model be subjected to the modification for shifting the chordwise C.G. mentioned above, two dummy blades were used in addition to the actual blade having variable chordwise C.G., as shown in Fig. 3.

The first test was conducted with the three-bladed rotor shown in Fig. 1. The shaft forward tilt angle was 10 degrees and the collective pitch

was set to 8 degrees at 75% radius location. The rotor rotational speed was 955 RPM (100 rad/sec) and the wind tunnel velocity was 30 MPH. At this point no gusts were applied in order to define the steady-state rotor motion. Then the vertical gust was applied to the rotor and the responses of the rotor were measured at gust frequencies of 100, 200, 300, 400, and 500 CPM. Having completed the 30 MPH sequence of the tests, the tunnel velocity was increased to 60 MPH and the same test sequence was followed as for 30 MPH. The results of these tests are described in Ref. 20. In general, they were similar to those for the single-bladed rotor.

The next portion of the test was with the single-bladed rotor with the tip weight shown in Fig. 3. The tungsten slug was positioned in the sleeve of the blade tip to place the chordwise center-of-gravity at 25% chord from the blade leading edge. It should be noted this C.G. location is the averaged one over the span. In this case the "stiff torsion" blade was used (the torsional natural frequency is 5.12/rev). The rotor had 8 degrees of collective pitch, the rotational speed was 955 RPM and the shaft tilt angle was 10 degrees. The same test sequence was followed as that of the three-bladed rotor, to measure the frequency response of the rotor to vertical gusts at advance ratios 0.192 and 0.384.

The tungsten slug was moved forward to place the chordwise C.G. location at 18% chord from the leading edge, and the gust frequency responses were measured. The slug was then moved backwards to obtain the chordwise C.G. location 35% chord from the leading edge, and the frequency responses were again measured. In the above cases the "stiff torsion" blade were used. The rotor blade remained stable in any C.G. location tested due to its very low Lock number.

The final part of the test used the "soft torsion" blade (the torsional natural frequency is 2.38/rev with 25% chord chordwise C.G. location from the leading edge) with variable C.G. location. The wind tunnel velocity was set to 30 MPH and 60 MPH. The chordwise C.G. location was varied 18%, 25% and 35% chord from the leading edge at both tunnel velocities, and the vertical gust was applied to the rotor.

3. Results and Discussion

Using the theory derived in Ref. 20, the blade chordwise center-of-gravity shift as a gust alleviation method is evaluated and the theory is compared with the experimental results. Rotor blade characteristics employed in this analysis are based on the wind tunnel model described in the previous section and detailed characteristics are listed in Table 1. In addition to the chordwise center-of-gravity shift as a principal parameter, the parameters examined in this analysis include cruising flight at advance ratios of 0.192 and 0.384, and blade torsional stiffness.

Based on the mass and stiffness distribution of the wind tunnel model blade, rotating blade natural frequencies and associated mode shapes were obtained from the theory developed in Ref. 20. Mode shapes of the blade with "stiff" torsional stiffness and C.G. at 25% chord from the leading edge are shown in Fig. 4.

Non-rotating natural frequencies for lag and torsion were determined experimentally with cantilevered hub restraint and compared to the calculated values. These are listed below. The non-rotating flap frequency was zero due to the blade flap hinge. Rotating blade natural frequencies were not obtained in the experiment.

WIND TUNNEL MODEL BLADE
NON-ROTATING NATURAL FREQUENCIES (Hz)

		LAG FREQUENCY		TORSIONAL FREQUENCY	
		EXPERIMENT	THEORY	EXPERIMENT	THEORY
THREE BLADED		9.1	9.15	109	113
SINGLE-BLADED WITH 25% C.G. FROM L.E.	STIFF TORSION	7.5	7.7	83	81.9
	SOFT TORSION	6.6	6.9	38	39.4

The output of the strain gage signals for the blade flap, lag and torsional motions were recorded on magnetic tape using a Hewlett Packard 4-channel Model 3960 tape recorder. These recorded data were fed to an analog-to-digital converter (Digital Equipment Corp. computer PDP-11/40) and 512 digital data points were sampled with a 6 msec sampling rate. This corresponds to 10.5 data points per rotor revolution. After sampling, data were digitally analyzed by Fast Fourier Transform (Ref. 22) with the same machine to obtain the frequency spectrum of the signal.

Sample analog data from the flap and torsion strain gages are shown in Fig. 5. The configuration is the three-bladed rotor with tunnel velocity 30 MPH and vertical gust frequency 200 CPM. From this analog data the frequency spectrum shown in Fig. 6 is obtained by the method mentioned above. The blade motion response to vertical gusts can be expressed in terms of the three frequency modulated motions ω, $(\Omega-\omega)$ and $(\Omega+\omega)$, where Ω is the rotational speed of the rotor and ω is the gust frequency. With reference to the blade flap frequency spectrum of Fig. 6, the first peak from the left is the response to the gust frequency ω, called the collective flapping response. The peak at the nondimensional frequency $\frac{\omega}{\Omega} = 0.791$ corresponds to the $(\Omega-\omega)$ cyclic flapping response. The big peak at $\frac{\omega}{\Omega} = 1.0$ has Ω frequency and comes from the steady state blade flapping motion due to forward flight. From the present linear theory 1Ω steady-state cyclic flapping motion is not affected by the vertical gust, and this is confirmed by the experimental results. The peak to the right of the Ω frequency response is the $(\Omega+\omega)$ cyclic flapping response.

The experimental results are compared to the theory in terms of the peak values of the blade motion frequency spectrum at frequencies ω, $(\Omega-\omega)$

and $(\Omega+\omega)$. For important responses such as blade flapping motion the frequency spectrum analysis was conducted several times on different portions of the magnetic tape on which analog signals from strain gages had been recorded for three minutes. This is a kind of averaging process because the total time required for sampling is 3.07 seconds from 3 minutes of data.

It is shown in the theoretical analysis of Ref. 20 how to obtain the three frequency-modulated responses ω, $(\Omega-\omega)$ and $(\Omega+\omega)$. However, it would be helpful to explain the method briefly here. The simplified blade flapping equation with vertical gust excitation may be written:

$$\ddot{\beta} + \{\frac{\gamma}{8} + \mu \frac{\gamma}{6} \sin(\Omega t)\} \dot{\beta} + \{(\frac{\omega_\beta}{\Omega})^2 + \mu \frac{\gamma}{6} \cos(\Omega t) + \mu^2 \frac{\gamma}{8} \sin(\Omega t)\} \beta = \frac{\gamma}{2} \int_0^1 x^2 w_G dx + \frac{\gamma}{2} \mu \sin(\Omega t) \int_0^1 x\, w_G\, dx \tag{1}$$

where

x = nondimensional radial coordinate

γ = Lock number

μ = advance ratio

ω_β = rotating flapping natural frequency

Ω = rotor rotational speed

t = time

w_G = vertical gust velocity nondimensionalized by blade tip speed (ΩR) at the radial coordinate x

As shown in Fig. 7, the one-dimensional sinusoidal gust in the cruising direction has a velocity gradient. The gust magnitude at the nondimensional spanwise location x of the blade of azimuth angle $\psi = \Omega t$ is expressed as:

$$w_G = \bar{w}_G \sin(\omega t - \phi_G) \tag{2}$$

where $\bar{w}_G$ is a gust amplitude and ω the gust frequency, ϕ_G phase lag of the gust between that location and the center of the rotor. The phase lag ϕ_G is described by the gust wave length λ_G and the location of the given point as:

$$\phi_G = 2\pi \frac{Rx \cos \Omega t}{\lambda_G} = \frac{1}{\mu} (\frac{\omega}{\Omega})\, x \cos \Omega t \tag{3}$$

Substituting Eq. 94 into Eq. 93 and expanding the trigonometric function yields:

$$w_G \approx \bar{w}_G \sin\omega t - \bar{w}_G \frac{x}{\mu}\frac{\omega}{\Omega}\cos\omega t \cos\Omega t \qquad + \text{Higher Order Terms}$$

$$= \bar{w}_G \sin\omega t - \frac{1}{2} w_G \frac{x}{\mu}\frac{\omega}{\Omega}[\cos(\Omega-\omega)t + \cos(\Omega+\omega)t] + \text{H.O.T.} \qquad (4)$$

In order to obtain the analytical excitation function, the approximate Eq. 4 is used instead of Eq. 2. The first term shows the uniform part of the gust and the second the gust velocity gradient due to the one-dimensional sinusoidal vertical gust.

The excitation function used in Ref. 6 is of the form

$$w_G = \bar{w}_G J_o(kx) \sin\omega t + \bar{w}_G J_1(kx) \cos(\Omega-\omega)t \qquad (5)$$

where $k = \frac{\omega}{\Omega}\frac{1}{\mu}$. If $kx < 1$,

$$J_o(kx) \approx 1$$

$$J_1(kx) \approx \frac{1}{2} kx = \frac{1}{2}\frac{x}{\mu}\frac{\omega}{\Omega}$$

and Equations 4 and 5 are roughly equivalent. Note, however, that the $\cos(\Omega+\omega)t$ term omitted in Eq. 5 is close to resonance with the first flapping mode of the rotor blade, and will amplify the blade response to the lower gust frequencies.

Substituting Equation 4 into Equation 1 yields (Left-hand side of Eq. 1)

$$= \frac{\gamma}{6}\bar{w}_G \sin\omega t + \frac{1}{2}\left\{\mu\frac{\gamma}{4} + \frac{1}{\mu}\frac{\gamma}{8}\left(\frac{\omega}{\Omega}\right)\right\}\bar{w}_G \cos(\Omega+\omega)t$$

$$+ \frac{1}{2}\left\{\mu\frac{\gamma}{4} - \frac{1}{\mu}\frac{\gamma}{8}\left(\frac{\omega}{\Omega}\right)\right\}\bar{w}_G \cos(\Omega-\omega)t \qquad + \text{Higher Order Terms} \qquad (6)$$

Therefore, due to the vertical gust with frequency ω, flapping motions of frequency ω, $(\Omega-\omega)$ and $(\Omega+\omega)$ are excited.

The effect of the inclusion of the gust velocity gradient due to the gust nonuniformity is shown in Fig. 8. Flap response levels are compared with and without the gust velocity gradient. It should be noted that the gust velocity gradient has a significant effect on the cyclic flapping motion even if the ratio of the wave length to the rotor radius is 11.

While the initial wind tunnel tests dealt with the gust response of the three-bladed rotor described in Ref. 20, the most important portion of the experiment involved the single-bladed rotor configuration with chordwise center-of-gravity shift. An objective of the test program was to evaluate the effectiveness of torsional stiffness variation in conjunction with chordwise center-or-gravity shifts in alleviating the gust response of a hingeless rotor. The comparison of the theoretical rotor responses with the experimental responses from the wind tunnel test will be discussed. The gust magnitudes used are shown in Fig. 9.

The gust responses for flap and torsion motions of the "stiff" and "soft" torsion blade in 30 MPH are shown in Fig. 10.

The flap motion response with "stiff torsion" blade are shown in Fig. 10(a). The $(\Omega+\omega)$ cyclic flapping response has a peak at frequency 0.15/rev. This is because the $(\Omega+\omega)$ cyclic flap motion is close to the blade rotating natural frequency. As expected, the flap response differences resulting from the chordwise center-or-gravity shift are very small, because the torsional motion produced by the C.G. shift was small due to the blade stiff torsional characterisitics. In addition to the blade stiff torsional characteristics, the Lock number for this single-bladed rotor is very low, having a value of 0.951. This is roughly one-tenth that of a full-scale helicopter and therefore the aerodynamic forces on this blade are one-tenth as effective in comparison with the aerodynamic forces on the full-scale helicopter. Therefore, the small angle of attack change due to the torsional motion did not produce effective aerodynamic forces to suppress or excite the flap motion. The torsional motion corresponding to the flap response in Fig. 10(a) is shown in Fig. 10(b).

When the "soft torsion" blade is utilized, larger flap response level differences due to chordwise C.G. shift at 30 MPH can be observed in Fig. 10(c). For the $(\Omega+\omega)$ cyclic and ω collective flap response it is clear that the experimental response of 18% chord C.G. location is lowest, that of 25% is in the middle and that of 35% is the highest. This tendency is the same as that of the theoretical prediction shown in Fig. 10(c). However, predicted response levels for a given C.G. location are higher than the experimental results location in the $(\Omega+\omega)$ and ω flapping responses. Corresponding to the flap response with "soft torsion" blade at 30 MPH are the torsional responses shown in Fig. 10(d), and good agreement is obtained between the theoretical prediction and experimental observation.

Lag motion responses at 30 MPH are shown in Fig. 10(e) and (f); they are very small.

The gust responses at 60 MPH are shown in Fig. 11. As with the 30 MPH case, chordwise center-of-gravity shifts for the "stiff torsion" blade did not produce distinctive flapping response reductions. Overall agreement between theoretical predictions and experimental results is good. The torsional responses of the "stiff torsion" blade at 60 MPH is shown in Fig. 11(b).

The flap responses with "soft torsion" blade at 60 MPH are shown in Fig. 11(c). While there is good agreement regarding the tendencies for the $(\Omega+\omega)$, ω, $(\Omega-\omega)$ flapping responses, the experimental magnitudes are slightly higher than those predicted, particularly the $(\Omega+\omega)$ and ω flap responses of 25 and 35% chordwise center-of-gravity cases. For the $(\Omega+\omega)$ cyclic flap response at the frequency $\omega/\Omega = 0.105$ the C.G. shift from 35% from the leading edge to 25% chord did increase the response level slightly in the experiment and no reduction can be seen in the theoretical prediction. At the same frequency the $(\Omega+\omega)$ cyclic flap response is reduced experimentally after shifting the C.G. forward from 25% to 18% chordwise station. From the theory, response reduction of the $(\Omega+\omega)$ cyclic flap response can be expected below the frequency $\omega/\Omega = 0.105$ shown in Fig. 11(c). This is an important point. The von Karman gust power spectral density scaled down to the present wind tunnel rotor model is shown in Fig. 12 where the gust characteristic length is 40 ft, V is 60 MPH and the model scaling factor is one-tenth. As is shown in Fig. 12 the gust power spectrum has a peak at the frequency $\omega/\Omega = 0.01$ and above $\omega/\Omega = 0.01$ it decays very rapidly. Therefore, the frequency response below a frequency ω/Ω of 0.1 is particularly important.

Above the frequency $\omega/\Omega = 0.157$ the $(\Omega+\omega)$ cyclic flap response reduction can be observed clearly in shifting from the 35% C.G. to 25% C.G., however, there is slight reduction from 25% C.G. to 18% C.G. in the experimental results. Experimental reductions of the ω collective flapping response is shown in Fig. 11(c).

Torsional responses are shown in Fig. 11(d) and good agreement between the theoretical predictions and the experimental results is obtained.

Lag responses are shown in Fig. 11(e) and (f). The theory predicts a lag resonance at the lag natural frequency and in the experiment it was not seen. It is not clear why this discrepancy exists. It may be due to experimental inaccuracy because the lag response level is very low.

Summarizing the rotor gust response, the gust velocity gradient due to the gust nonuniformity over the rotor disc has an important role in the blade cyclic motion responses unless the gust frequency is extremely low.

The frequency response of blade motion to a vertical gust with frequency ω is described in terms of three frequency-modulated motions at ω, $(\Omega-\omega)$ and $(\Omega+\omega)$, where Ω is the rotational speed. The responses $(\Omega-\omega)$ and $(\Omega+\omega)$ are related to the blade cyclic motions. Therefore, even if the gust frequency ω is low, the response close to 1/rev will be excited as $(\Omega+\omega)$ and $(\Omega-\omega)$ responses.

As expected, the "soft torsion" blade is more effective in conjunction with the forward chordwise center-of-gravity shift in alleviating the gust response of a hingeless rotor than the "stiff torsion" blade.

It should be mentioned that rotor rotational speed fluctuations were not considered in the analysis. However, these were found experimentally to be less than plus or minus three percent.

It should be noted that greater effectiveness of the chordwise center-of-gravity shift can be expected in the full size rotor since the present wind tunnel model rotor has very low Lock number.

The theoretical gust response of the hingeless rotor with Lock number 10 is shown in Fig. 13. The structural characteristics of the rotor blade are the same as those of the single-bladed rotor with tip mass used in the wind tunnel. The "soft torsion" blade, ω_ϕ/Ω = 2.38/rev, is employed. Blade density is reduced to obtain a typical full-size blade Lock number. The chordwise center-of-gravity is varied over 18%, 25% and 35% chord from the blade leading edge. For the 35% chord C.G. location, classical flap-torsion flutter occurred. The gust magnitude in Fig. 9 is used for the case μ = 0.384.

It is shown in Fig. 13 that the center-of-gravity shift is a very effective method to reduce the flapping response due to the greater aerodynamic forces in the full size rotor. It is interesting that the peak at 0.2/rev in the $(\Omega+\omega)$ flap response is reduced because of the large aerodynamic damping in the flapping motion. The ω flap response is higher than the cyclic flapping responses since the gust effectiveness has increased through the Lock number. In the $(\Omega-\omega)$ flap response the response of the 25% chord C.G. is less than that of the 18% chord C.G. at the gust frequency 0.4 because the phase of the torsional motion is not such as to reduce the flapping motion.

In this paper the blade flapping response was chosen as a measure of the effectiveness of the gust alleviation system. Therefore, the appropriateness of the flapping response as a measure was examined by evaluating the vertical shear force at the blade root, and also the blade root bending moment.

The vertical shear force at the root is obtained by integrating the aerodynamic and inertial forces of the blade:

$$S = \int_0^R (p_z - m\ddot{z})dr \qquad (7)$$

The harmonic balance method was applied to eliminate the periodic coefficients, and the shear force was expressed in terms of ω, $(\Omega-\omega)$ and $(\Omega+\omega)$ vibratory shear forces. Both first and second mode flapping motions were included.

The results shown in Fig. 14 are the calculated shear forces due to gusts of the single-bladed model rotor with the "soft torsion" blade at advance ratio 0.394 with chordwise center-of-gravity shift. Note that the shear force components at frequencies ω, $(\Omega-\omega)$, and $(\Omega+\omega)$ are reduced by shifting the chordwise center-of-gravity forward. The flapping responses corresponding to these shear forces are shown in Fig. 10(c) and it is obvious that the flapping may be taken as a measure of the effectiveness of the gust alleviation system in reducing hub shears. In the present wind tunnel model, the hub moment is expressed in terms of the product of the vertical shear force and the flap hinge offset. Therefore, the hub moment is proportional to the shear force and the hub moment is also reduced by forward C.G. shift. It can be concluded that the first mode flapping motion may be chosen as an indicator of the effectivenss of the gust alleviation system.

It should be noted that careful choice of blade mass balance spanwise location and blade torsional frequency are necessary to avoid possible amplification of hub shears due to higher harmonic airloads, as discussed in Reference 16.

4. Conclusions

This study has been devoted to the experimental verification of a theoretical model of hingeless rotor response to a vertical gust, and to the theoretical and experimental evaluation of the effect of shift of blade chordwise center-of-gravity as a gust alleviation method, particularly to reduce the blade flap motion.

Based upon the theoretical and experimental results in this study, the following conclusions may be stated:

(a) Chordwise center-of-gravity shift is an effective method of alleviating hingeless rotor gust response. It was experimentally confirmed that the flap response was reduced when the chordwise center-of-gravity was shifted toward the leading edge and the "soft torsion" blade was employed, for gust frequencies up to $\omega/\Omega = 0.5$. C.G. shift will therefore also reduce the response due to the discrete gust which has higher frequency content than random turbulence.

The full size blade with Lock number of order 10 shows even larger reductions of flapping response because of greater aerodynamic effectiveness.

(b) The "soft torsion" blade is more effective in conjunction with the forward chordwise center-of-gravity shift in alleviating the gust response than the "stiff torsion" blade.

(c) The agreement between the experimental gust response of the hingeless rotor and the theoretical predictions is good, particularly in the case of flapping and torsional motion.

(d) The frequency response of blade motion to a vertical gust with gust frequency ω is described in terms of motions at the frequencies ω, $(\Omega-\omega)$ and $(\Omega+\omega)$, where Ω is the rotor rotational speed. The responses at the frequency $(\Omega-\omega)$ and $(\Omega+\omega)$ will be excited even if the gust frequency ω is low.

(e) The gust velocity gradient due to the gust nonuniformity over the rotor disc has a significant effect on the blade response unless the wave length of the gust is extremely large with respect to the rotor diameter.

References

1) Gaonkar, G.H. and Hohenemser, K.H., "Stochastic Properties of Turbulence Excited Rotor Blade Vibrations", AIAA Journal, 9, 3, March 1971.

2) Gaonkar, G.H., Hohenemser, K.H. and Yin, S.K., "Random Gust Response Statistics for Coupled Torsion-Flapping Rotor Blade Vibrations", J. Aircraft, 9, 10, Oct. 1972.

3) Wan, F.Y.M. and Lakshmikantham, C., "Rotor Blade Response to Random Loading: Direct Time Domain Approach", AIAA Journal, 11, 1, Jan. 1973.

4) Wan, F.Y.M. and Lakshmikantham, C., "The Special Correlation Method and a Time Varying Flexible Structure", AIAA Paper 73-406, March 1973.

5) Archidacono, P.J., Bergquist, R.R. and Alexander, W.T., Jr., "Helicopter Gust Response Characteristics Including Unsteady Aerodynamic Stall Effects", Proceedings of Specialists Meeting on Rotorcraft Dynamics, NASA SP-352, Feb. 1974.

6) Judd, M. and Newman, S.J., "An Analysis of Helicopter Rotor Response Due To Gusts and Turbulence", Vertica, 1, 3, 1977.

7) Johnson, W., "Dynamics of Tilting Proprotor Aircraft in Cruise Flight", NASA TN D-7677, May 1974.

8) Yasue, M., "A Study of Gust Response for a Rotor-Propeller in Cruising Flight", Massachusetts Institute of Technology, Aeroelastic and Structures Research Laboratory, NASA CR-137537, Aug. 1974.

9) Johnson, W., "Analytical Model for Tilting Proprotor Aircraft Dynamics, Including Blade Torsion and Coupled Bending Modes, and Conversion Mode Operation", NASA TM X-62369, Aug. 1974.

10) Frick, J.K. and Johnson, W., "Optimal Control Theory Investigation of Proprotor/Wing Response to Vertical Gust", NASA TM X-62384, Sept. 1974.

11) Ham, N.D., Bauer, P.H., Lawrence, T.H. and Yasue, M., "A Study of Gust and Control Response of Model Rotor-Propellers in a Wind Tunnel Airstream", Massachusetts Institute of Technology, Aeroelastic and Structures Research Laboratory, NASA CR-137756, Aug. 1975.

12) Whitaker, H.P. and Cheng, Y., "Use of Active Control Systems to Improve Wing Bending and Rotor Flapping Responses of a Tilt Rotor VTOL Airplane", Massachusetts Institute of Technology, Aeroelastic and Structures Research Laboratory, ASRL TR 183-1, Oct. 1975.

13) Cheng, Y., "Application of Active Control Technology to Gust Alleviation System for Tilt Rotor Aircraft", Massachusetts Institute of Technology, Aeroelastic and Structures Research Laboratory, NASA CR-137958, Nov. 1976.

14) Miller, R.H., "A Method for Improving the Inherent Stability and Control Characteristics of Helicopters", Journal of the Aeronautical Sciences, 17, 6, June 1950, pp. 363-374.

15) Hirsh, H., Hutton, R.E. and Rasumoff, A., "Effect of Spanwise and Chordwise Mass Distribution on Rotor Blade Cyclic Stresses", Journal of American Helicopter Society, 1, 2, April 1956.

16) Miller, R.H. and Ellis, C.W., "Helicopter Blade Vibration and Flutter", Journal of American Helicopter Society, 1, 3, July 1956.

17) Reichert, G. and Oelker, P., "Handling Qualities with the Bolkow Rigid Rotor System", 24th Annual National Forum Proceedings of the American Helicopter Society, No. 218, May 1968.

18) Huber, H., "Some Objectives in Applying Hingeless Rotors to Helicopters and V/Stol Aircraft", AGARD CP-111, Sept. 1972.

19) Reichert, G. and Huber, H., "Influence of Elastic Coupling Effects on the Handling Qualities of a Hingeless Rotor Helicopter", AGARD CP-121, Feb. 1973.

20) Yasue, M., "Gust Response and Its Alleviation for a Hingeless Helicopter Rotor in Cruising Flight", Massachusetts Institute of Technology, Aeroelastic and Structures Research Laboratory, ASRL TR 189-1, Sept. 1978.

21) Biggers, J.C., "Some Approximations to the Flapping Stability of Helicopter Rotors", Journal of the American Helicopter Society, 19, 4, Oct. 1974.

22) Rabiner, L.R. and Gold, B., Theory and Application of Digital Signal Processing, Prentice-Hall, 1975.

TABLE 1

DESCRIPTION OF THE ROTOR BLADE
USED IN THE WIND TUNNEL TEST

	THREE-BLADED ROTOR	SINGLE-BLADED ROTOR WITH TIP WEIGHT AND 25% CHORD C.G. LOCATION FROM LEADING EDGE
Number of blades	3	1
Radius, R	2.26 ft	2.26 ft
Chord, C	2 in	2 in
Lock number, γ (basic configuration)	2.27	0.954
Solidity, σ	0.0704	0.0235
Collective pitch, θ_o	8 deg	8 deg
Shaft tilt angle in crusing flight	10 deg forward	10 deg. forward
Lift-curve slope, a	5.7	5.7
Drag coefficient, Cd_o	0.012	0.012
Rotational speed, Ω	100 rad/sec	100 rad/sec
Built-in blade angle of twist, θ_{TW}	8 deg (linear)	6 deg (linear)
Elastic axis	25% chord	25% chord
Aerodynamic center	25% chord	25% chord
Precone, β_p	0 deg	0 deg
Droop, δ_D	0 deg	0 deg
Torque offset, e_o	0 in	0 in
Control linkage flexibility	rigid	rigid
Basic Natural Frequencies		
Lag	0.823/rev	0.57/rev
Flap	1.13/rev	1.13/rev
Torsion	6.85/rev	5.21/rev (stiff) 2.38/rev (soft)

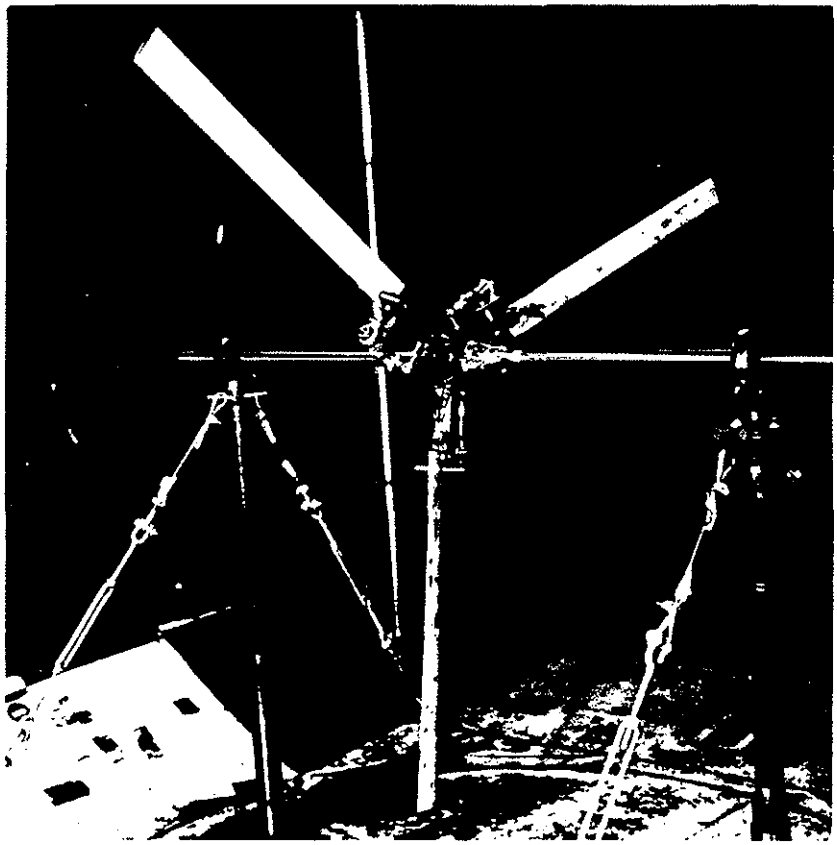

FIG. 1 THREE-BLADED ROTOR

FIG. 2 ROTOR BLADE FLEXURE, STRAIN GAGES,

AND LEAD-LAG DAMPER

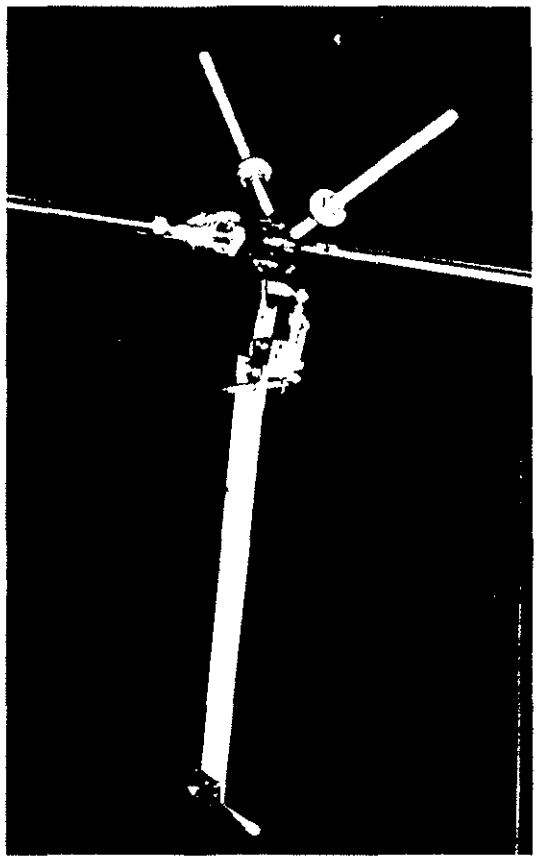

FIG. 3 SINGLE-BLADED ROTOR WITH TIP WEIGHT

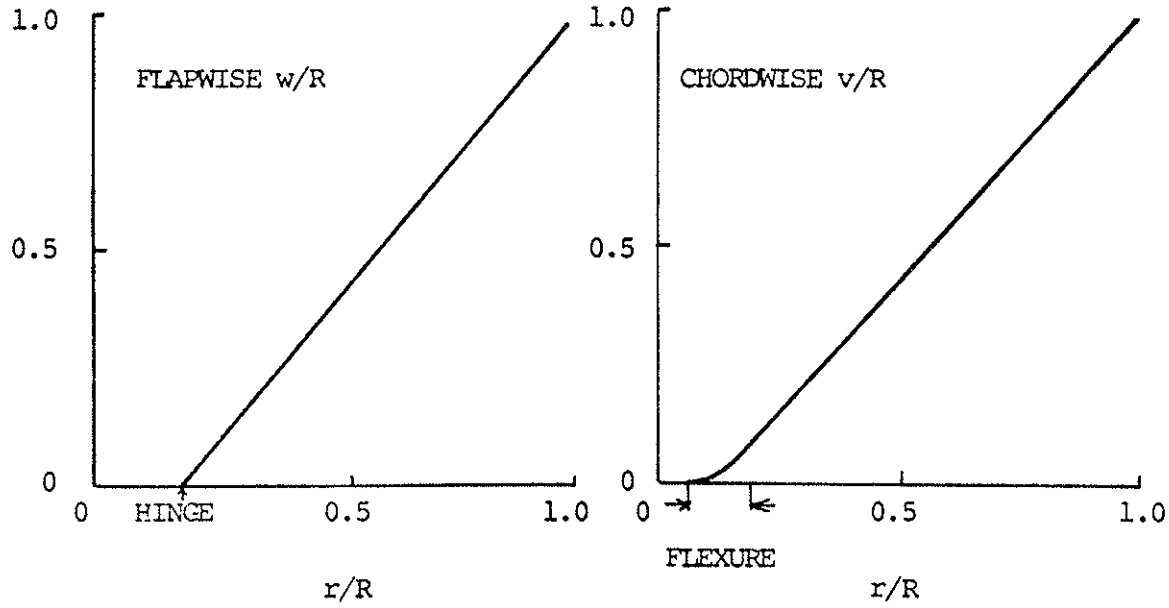

NATURAL FREQUENCY 1.13/rev

NATURAL FREQUENCY 0.82/rev

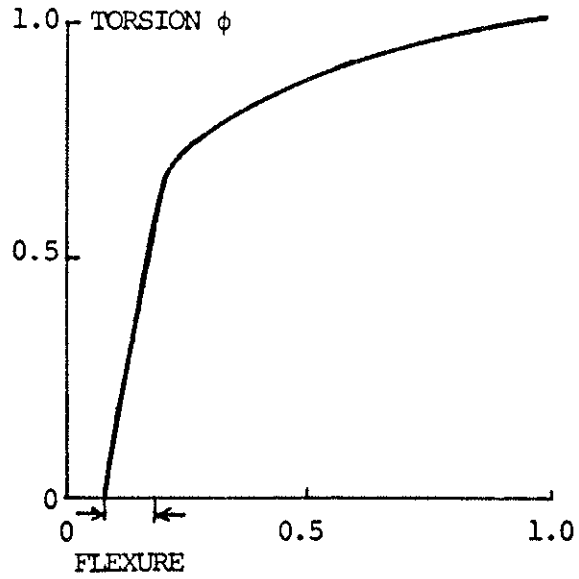

NATURAL FREQUENCY 6.85/rev

FIG. 4 MODE SHAPES OF THE WIND TUNNEL MODEL BLADE (THREE-BLADED ROTOR)

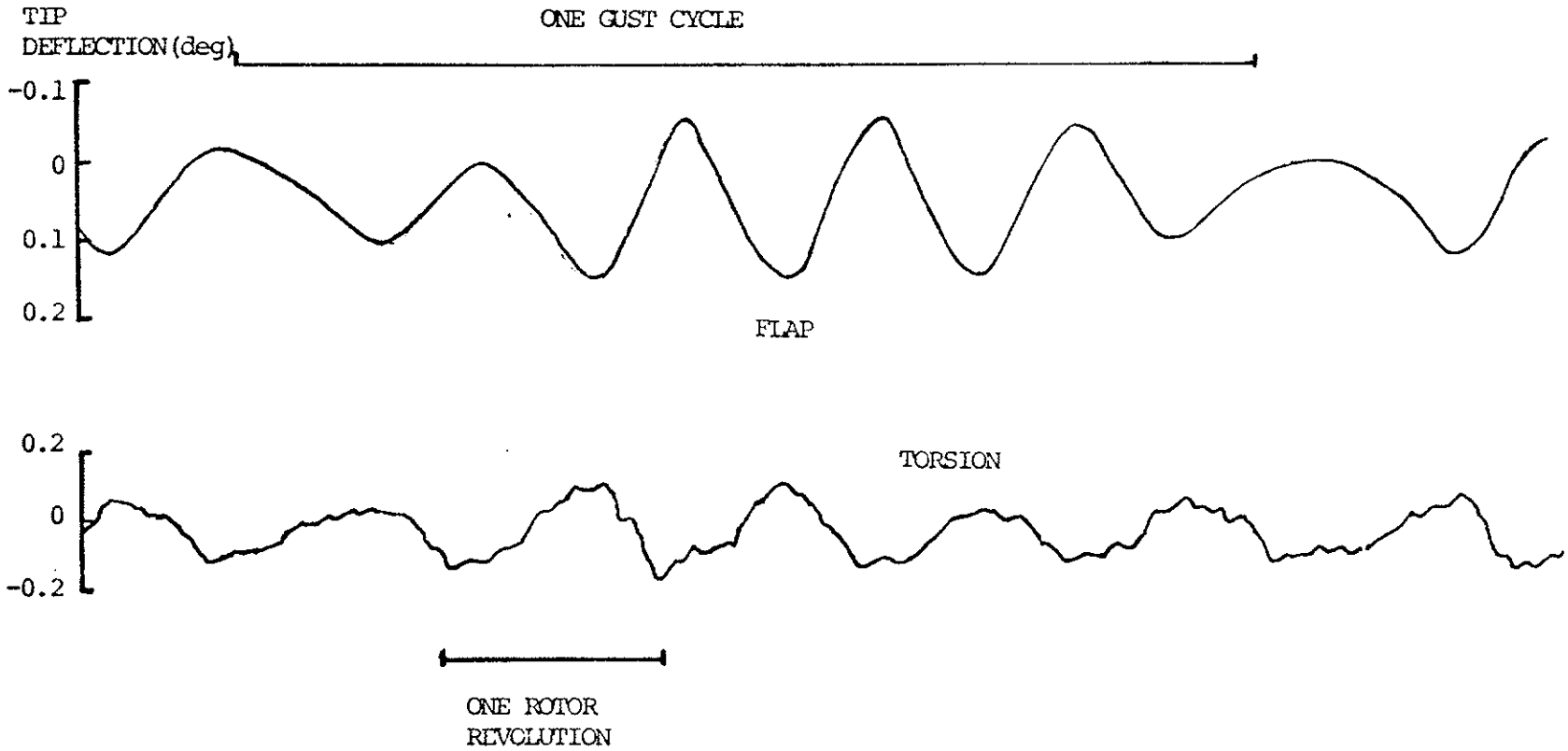

FIG. 5 TYPICAL TIME HISTORY OF THE VERTICAL GUST RESPONSES OF FLAP AND TORSION MOTIONS: THREE-BLADED ROTOR, μ=0.192 AND NONDIMENSIONAL GUST FREQUENCY ω/Ω=0.209

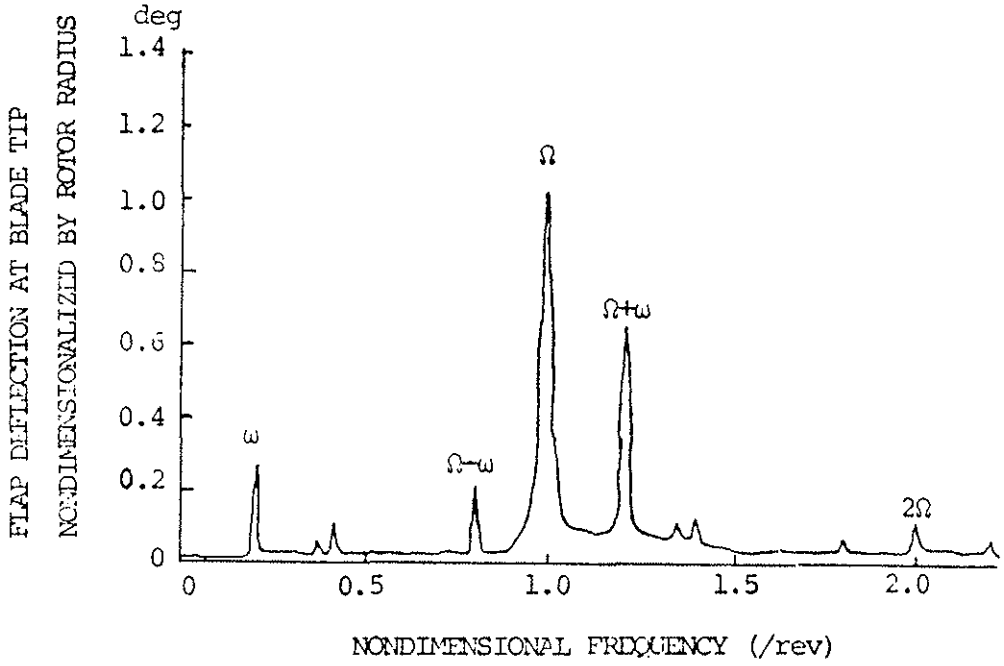

(a) FLAP RESPONSE

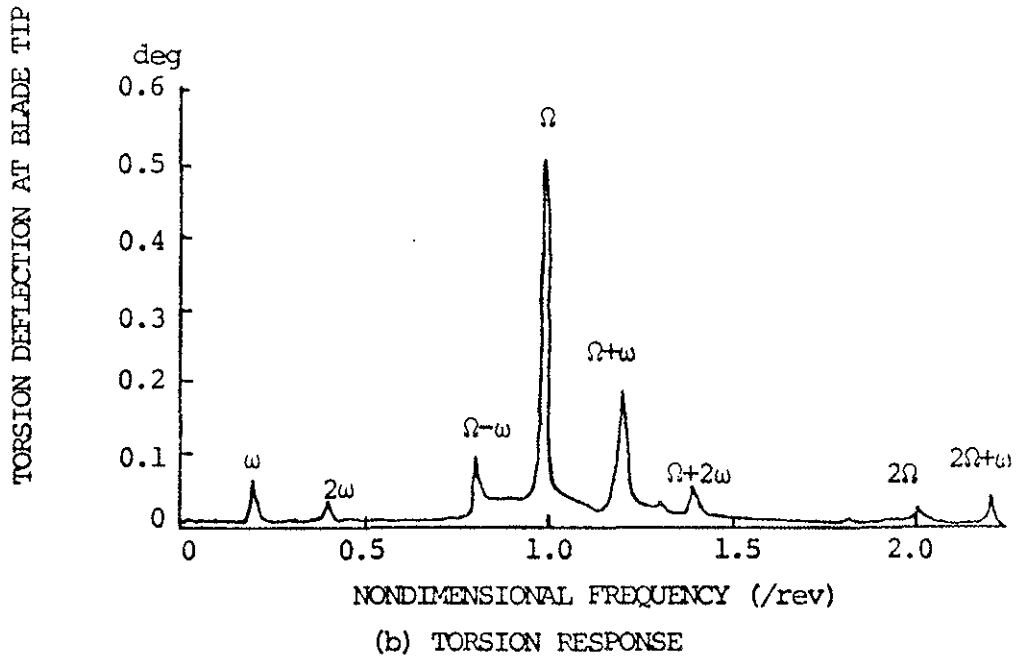

(b) TORSION RESPONSE

FIG. 6 TYPICAL FREQUENCY SPECTRUM OF THE VERTICAL GUST RESPONSES OF FLAP AND TORSION MOTIONS: THREE-BLADED ROTOR WITH GUST FREQUENCY $\omega/\Omega=0.209$ AT $\mu=0.192$

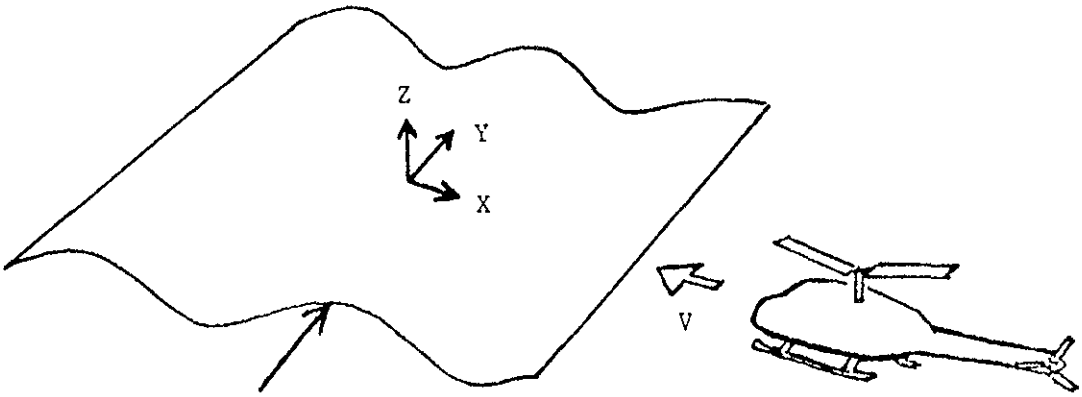

ONE DIMENSIONAL SINUSOIDAL
VERTICAL GUST

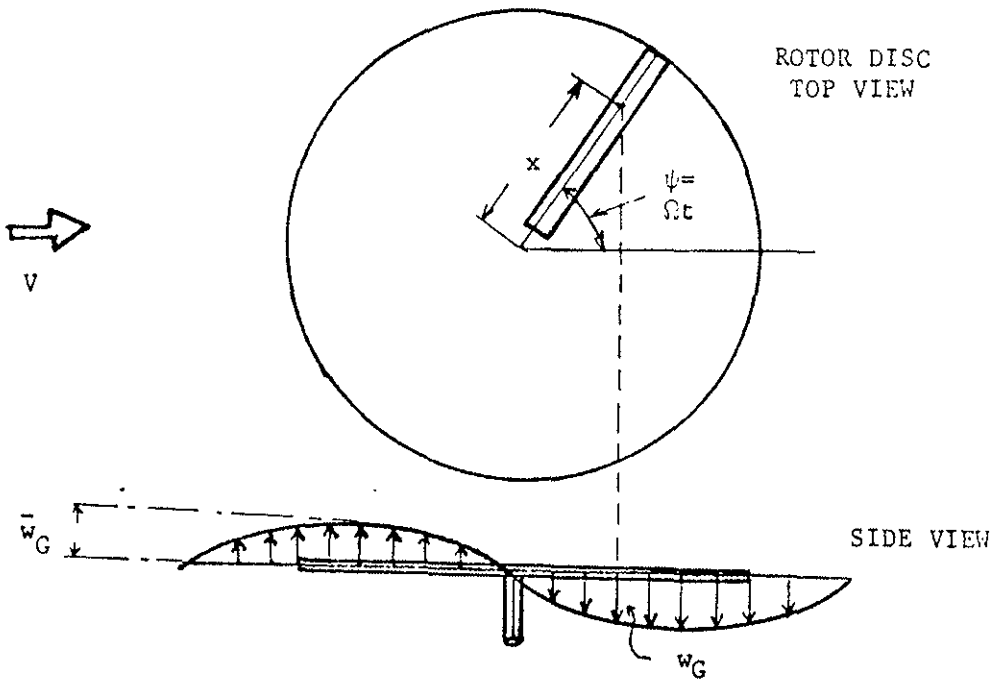

FIG. 7 GUST VELOCITY GRADIENT DUE TO GUST NONUNIFORMITY OVER THE ROTOR DISC

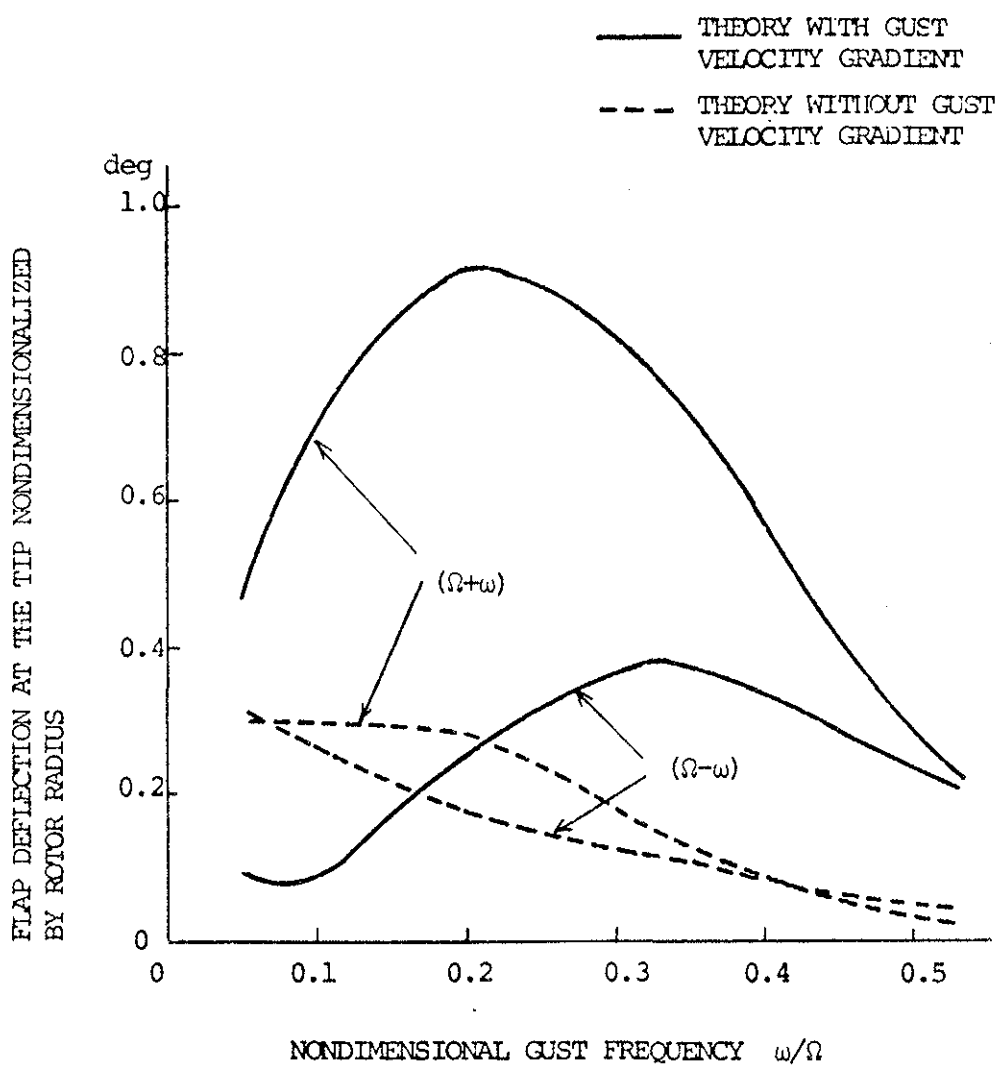

FIG. 8 EFFECT OF GUST VELOCITY GRADIENT ON THE FLAP RESPONSE: $\mu = 0.192$

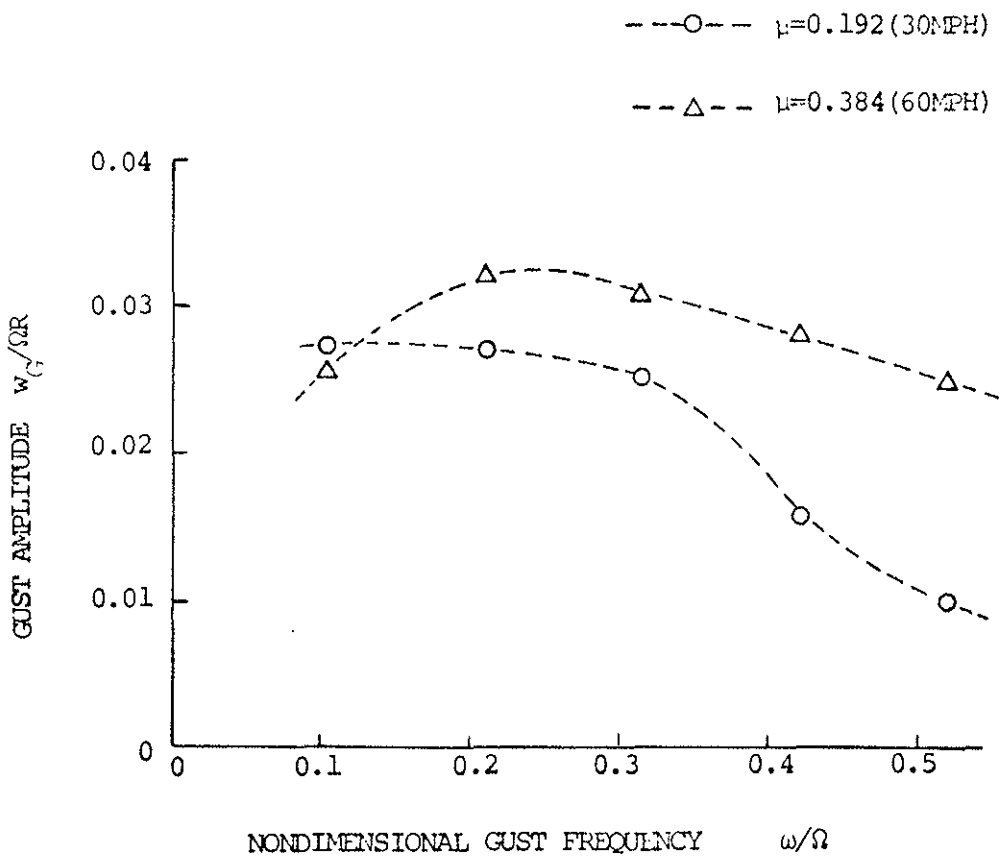

FIG. 9 VERTICAL GUST AMPLITUDE AT THE CENTER OF THE ROTOR DISC

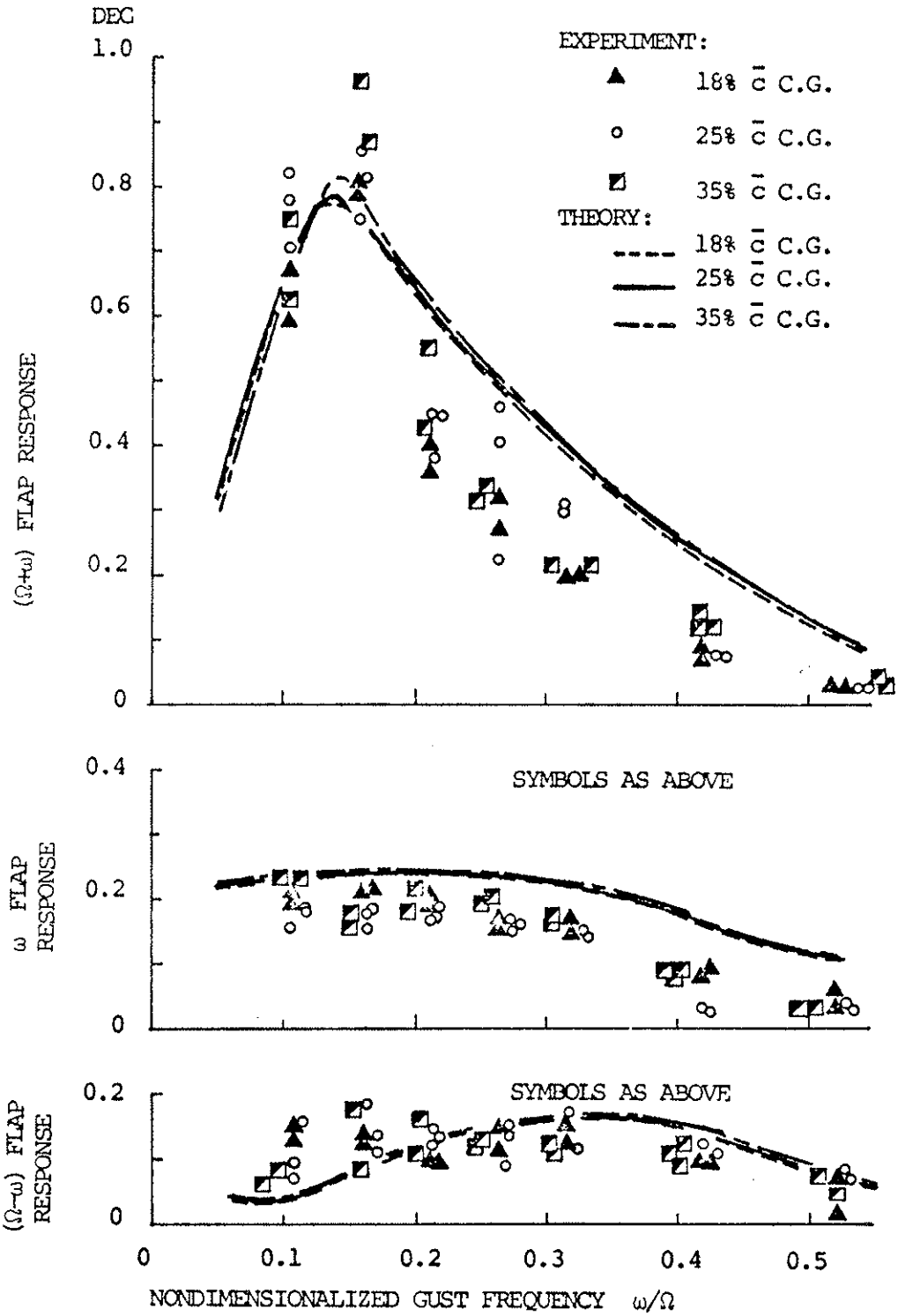

(a) FLAP RESPONSE OF "STIFF TORSION" BLADE: $\omega_\phi/\Omega = 5.21$ / rev

FIG. 10 SINGLE-BLADED ROTOR VERTICAL GUST RESPONSE AT ADVANCE RATIO 0.192 WITH CHORDWISE C.G. SHIFT. NOTE: FLAP AND LAG RESPONSES ARE EXPRESSED IN TERMS OF TIP DEFLECTION NONDIMENSIONALIZED BY RADIUS. TORSION IN TERMS OF TIP DEFLECTION

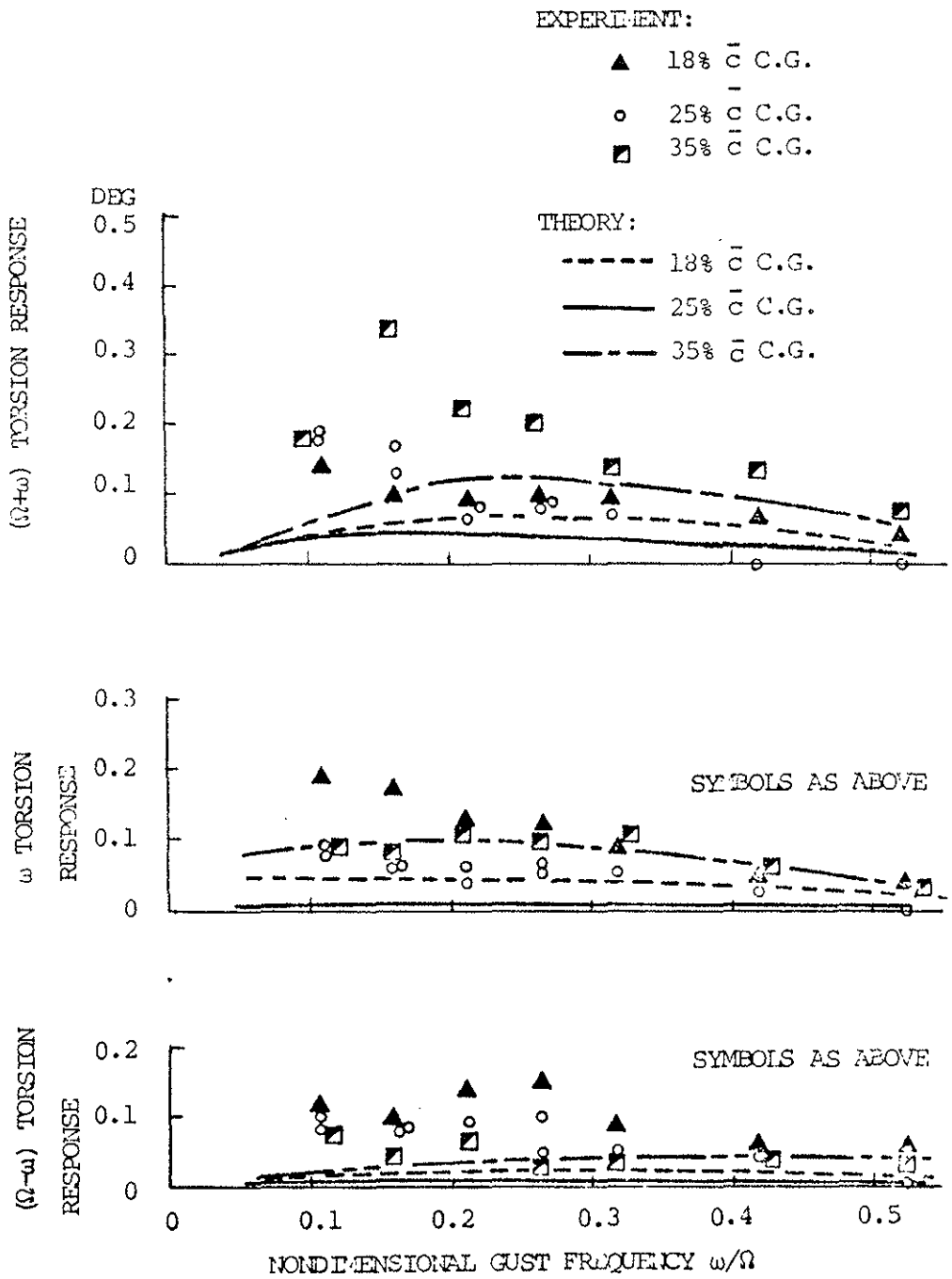

(b) TORSION RESPONSE OF "STIFF TORSION" BLADE: ω_ϕ/Ω=5.21/rev

FIG. 10 CONTINUED

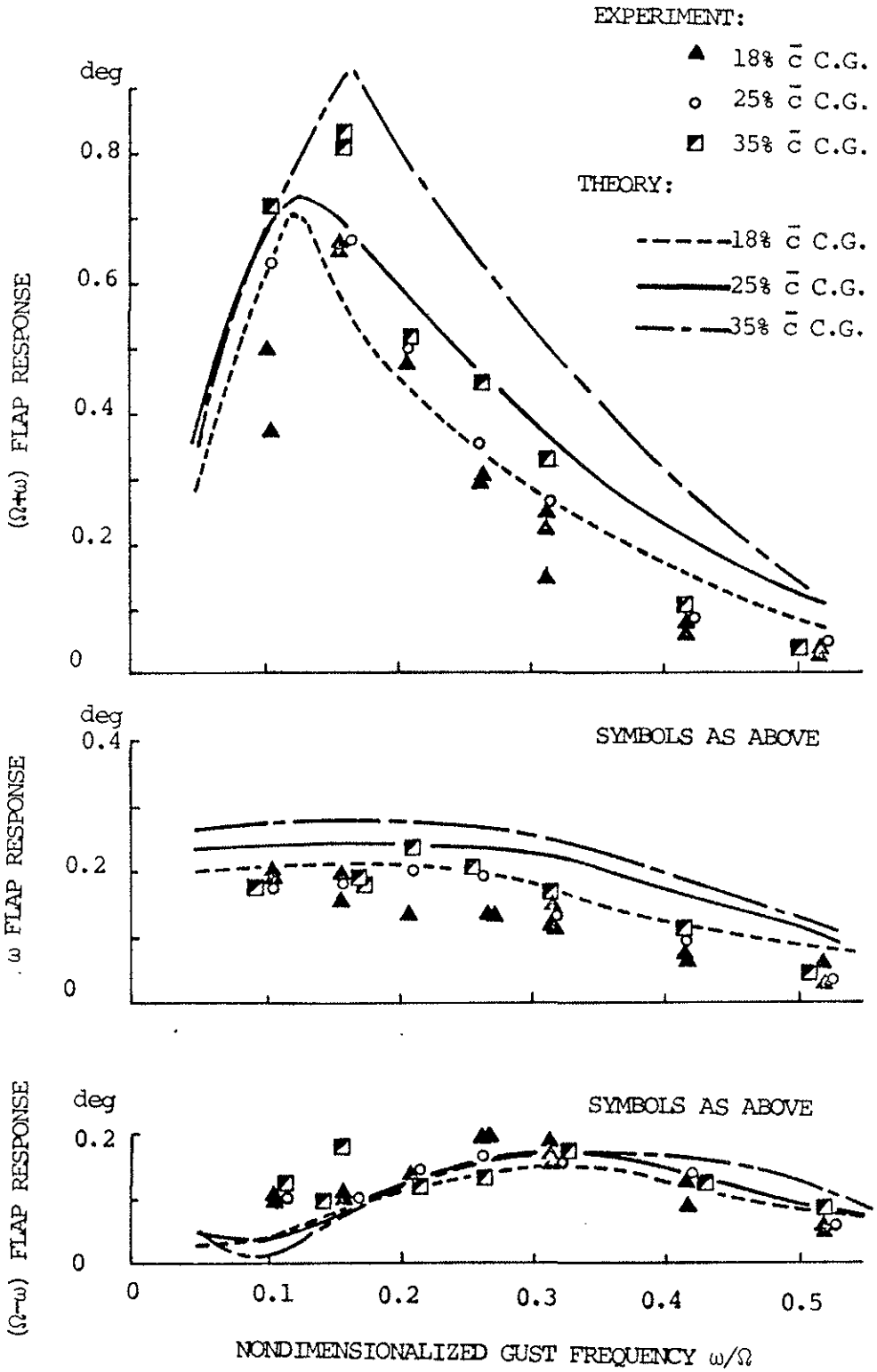

(c) FLAP RESPONSE OF " SOFT TORSION " BLADE: $\omega_\phi / \Omega = 2.38$ / rev

FIG. 10 CONTINUED

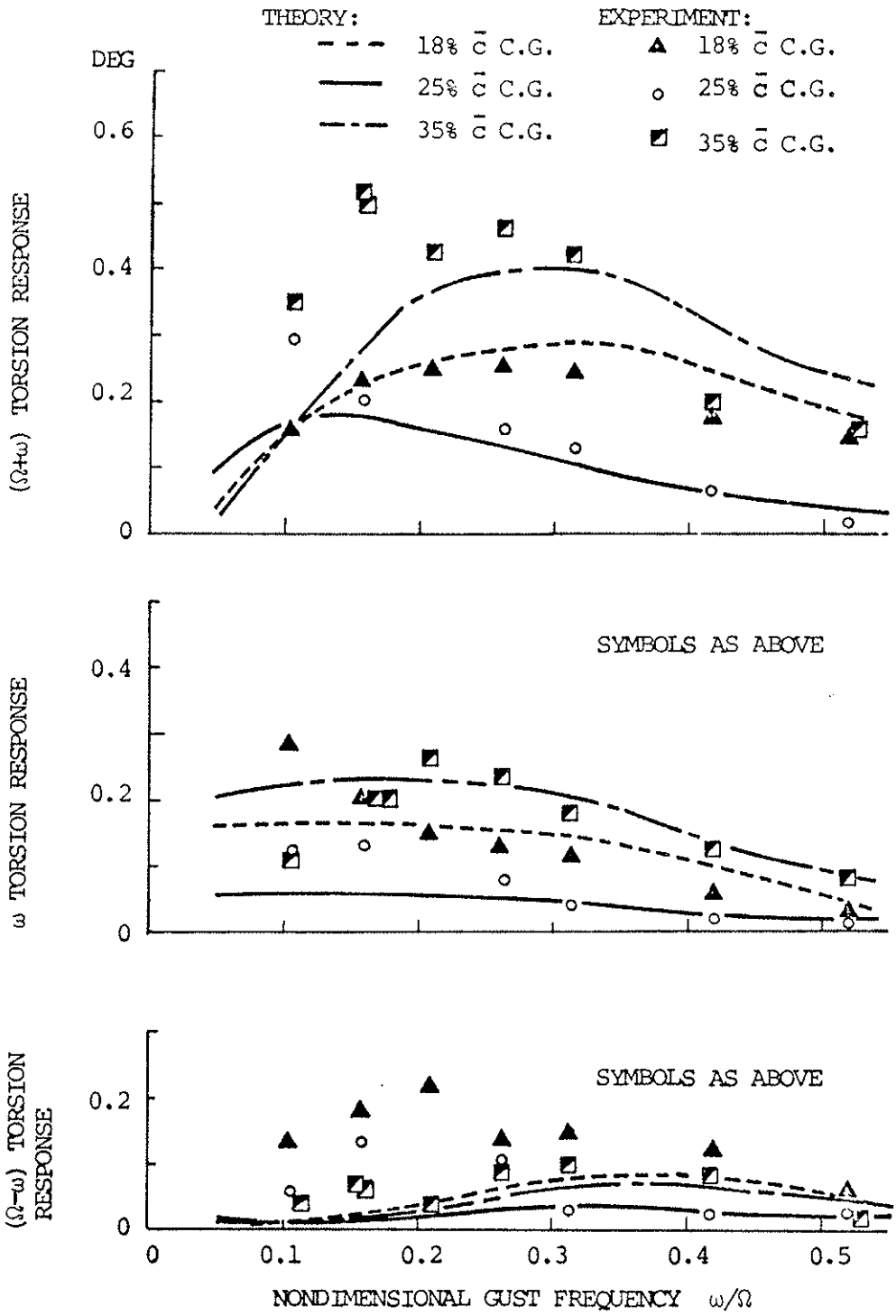

(d) TORSION RESPONSE OF "SOFT TORSION" BLADE: ω_ϕ/Ω=2.38/rev

FIG. 10 CONTINUED

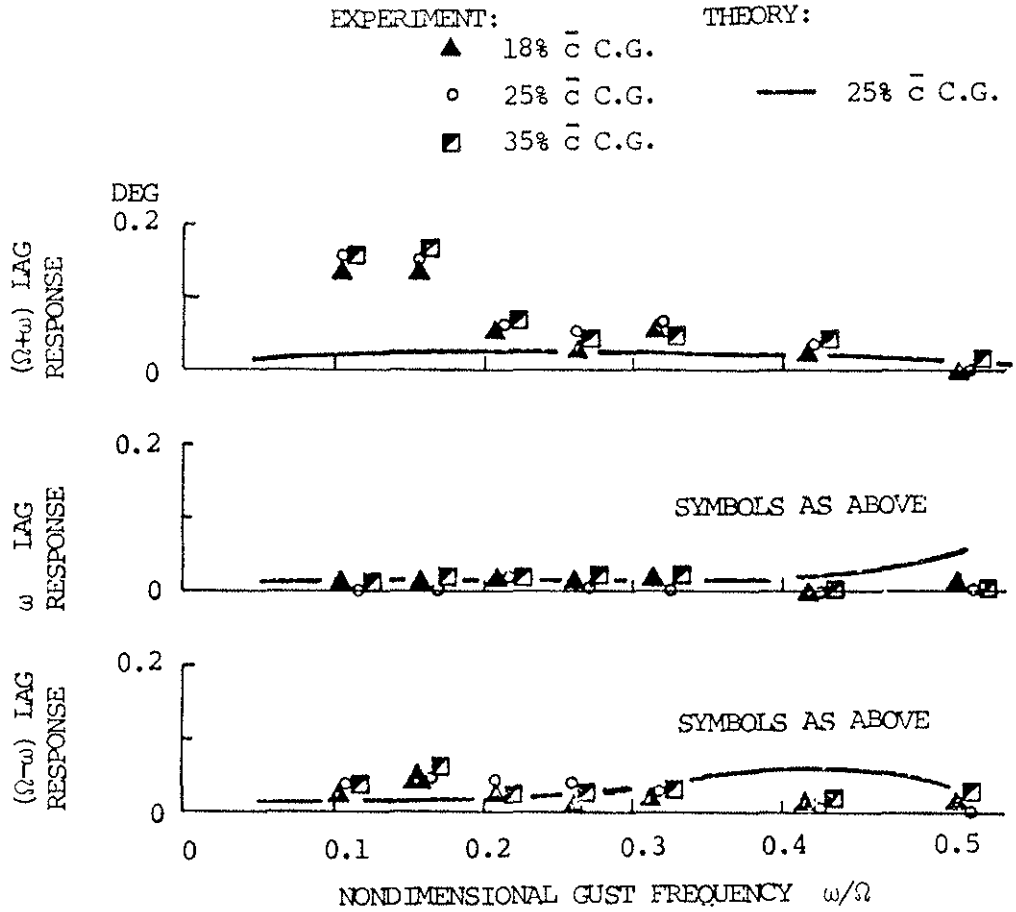

(e) LAG RESPONSE OF "STIFF TORSION" BLADE: ω_ϕ/Ω =5.21/rev

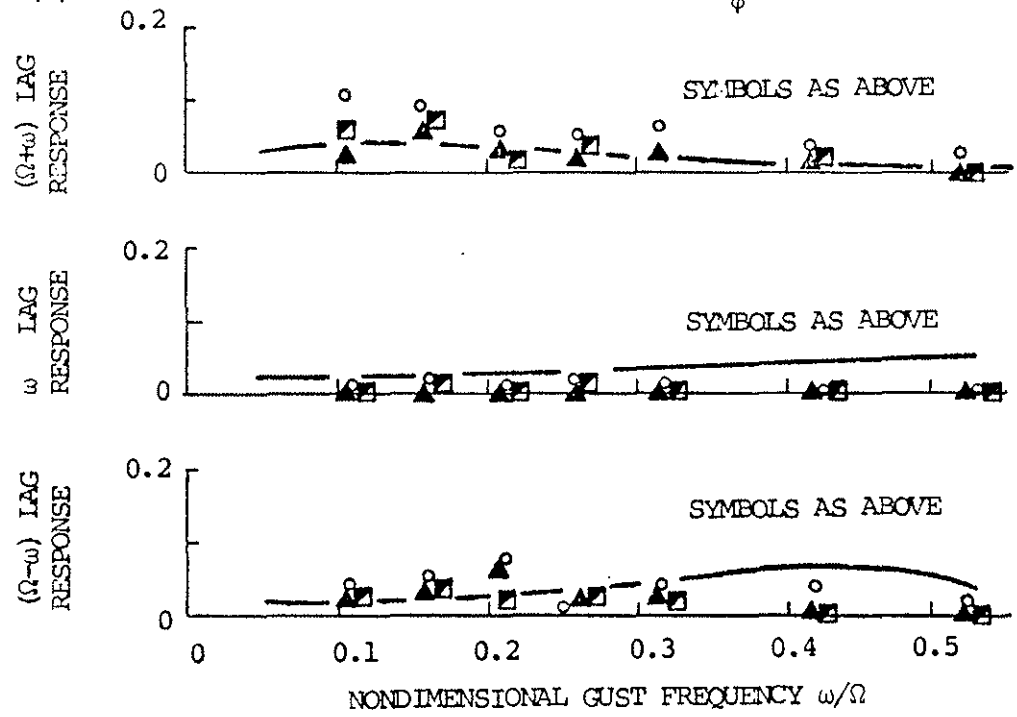

(f) LAG RESPONSE OF "SOFT TORSION" BLADE: ω_ϕ/Ω=2.38/rev

FIG. 10 CONCLUDED

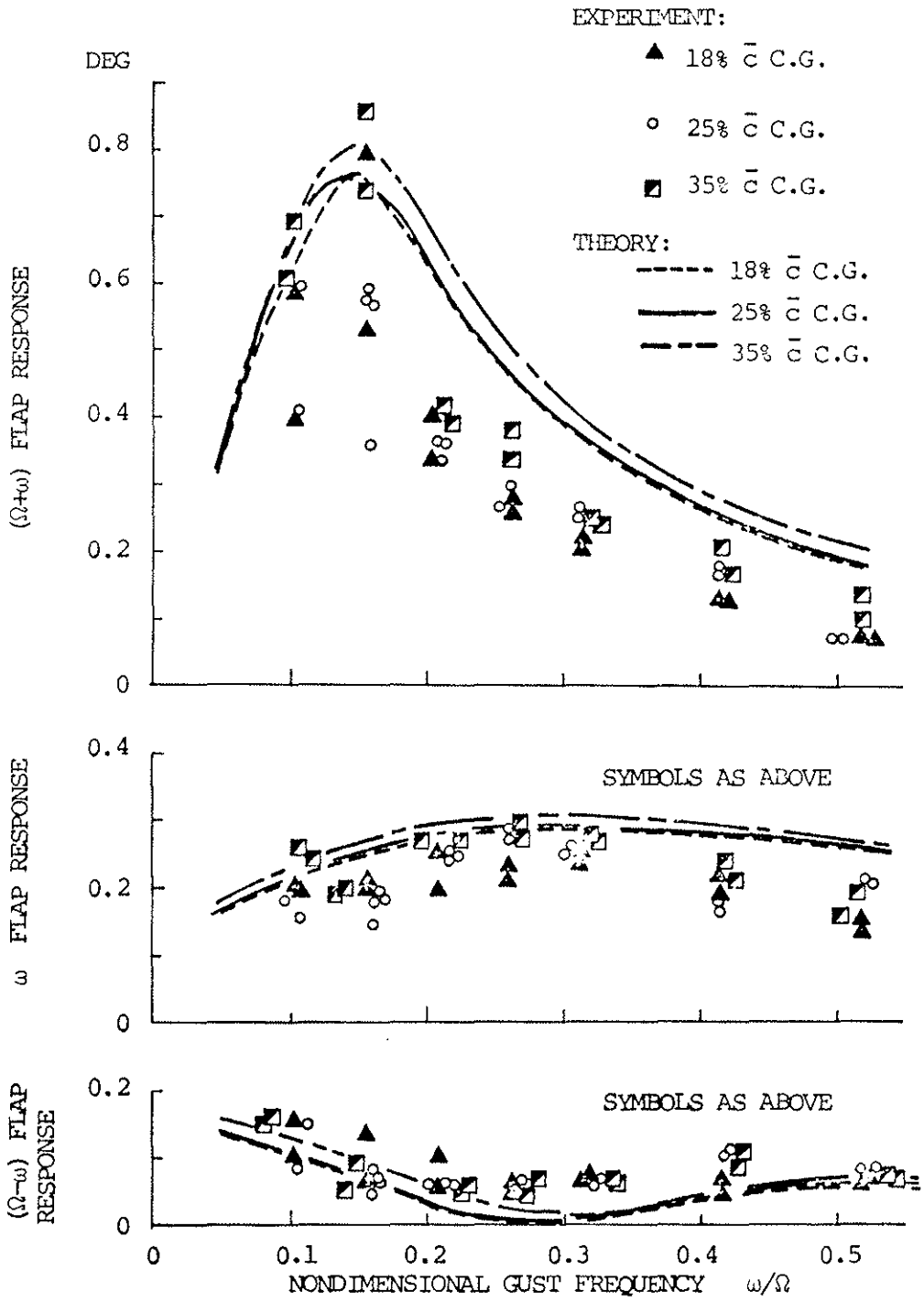

(a) FLAP RESPONSE OF "STIFF TORSION" BLADE: $\omega_\phi/\Omega=5.21/\text{rev}$

FIG. 11 SINGLE-BLADED ROTOR VERTICAL GUST RESPONSE AT ADVANCE RATIO 0.384 WITH CHORDWISE CENTER-OF-GRAVITY SHIFT. NOTE: FLAP AND LAG RESPONSES ARE EXPRESSED IN TERMS OF TIP DEFLECTION NONDIMENSIONALIZED BY RADIUS. TORSION IN TERMS OF TIP DEFLECTION.

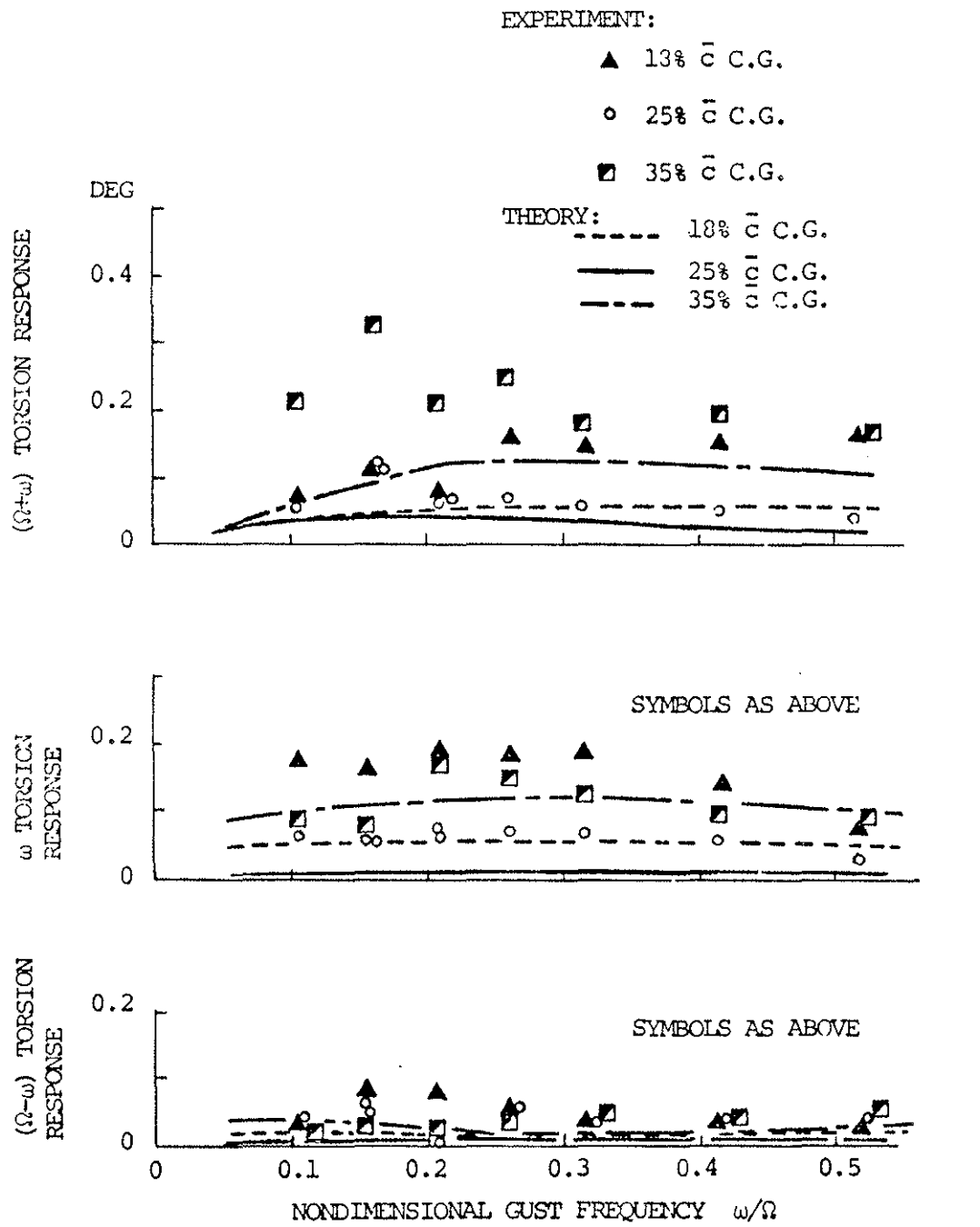

(b) TORSION RESPONSE OF "STIFF TORSION" BLADE: ω_ϕ/Ω=5.21/rev

FIG. 11 CONTINUED

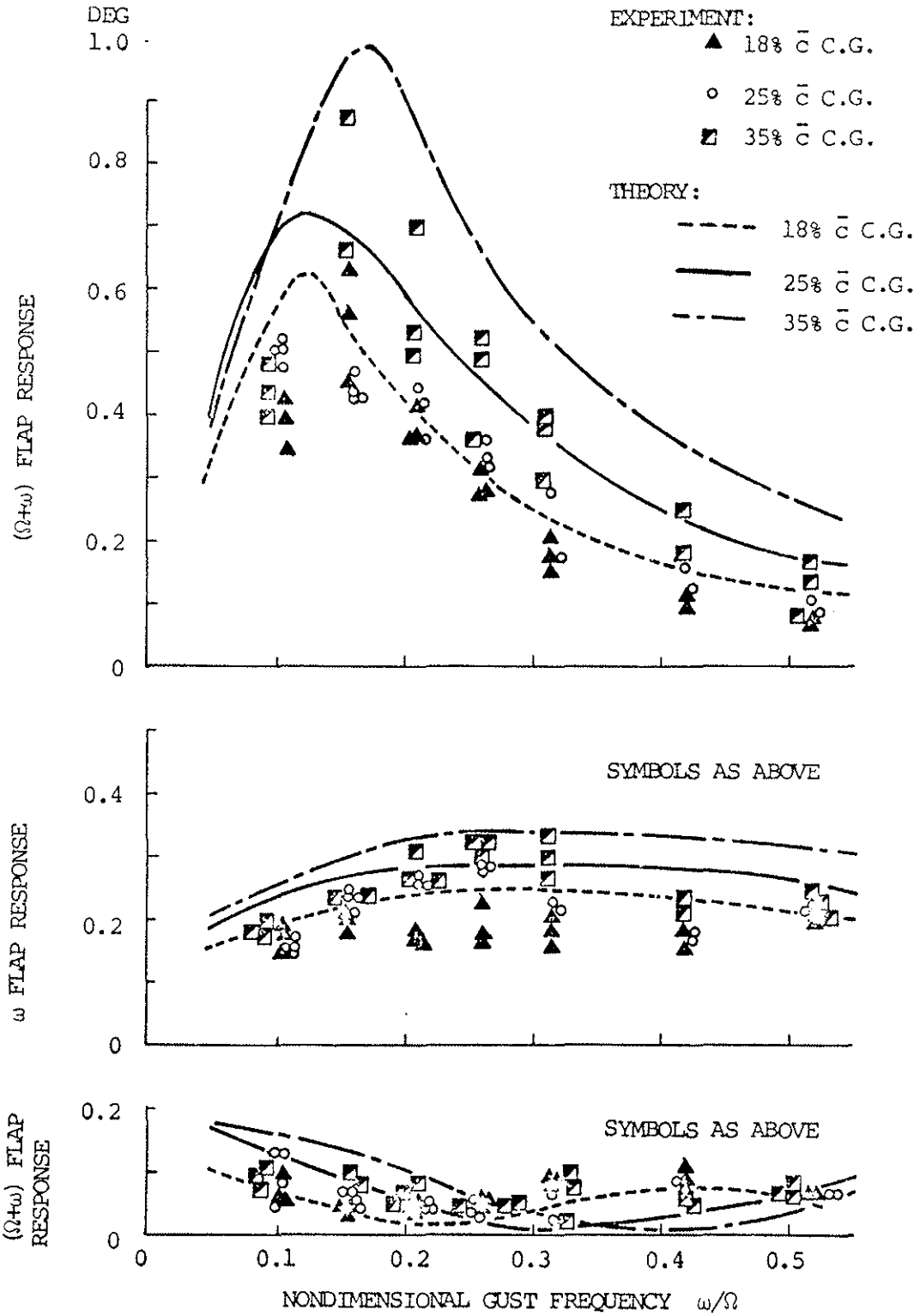

(c) FLAP RESPONSE OF "SOFT TORSION" BLADE: ω_ϕ/Ω=2.38/rev

FIG. 11 CONTINUED

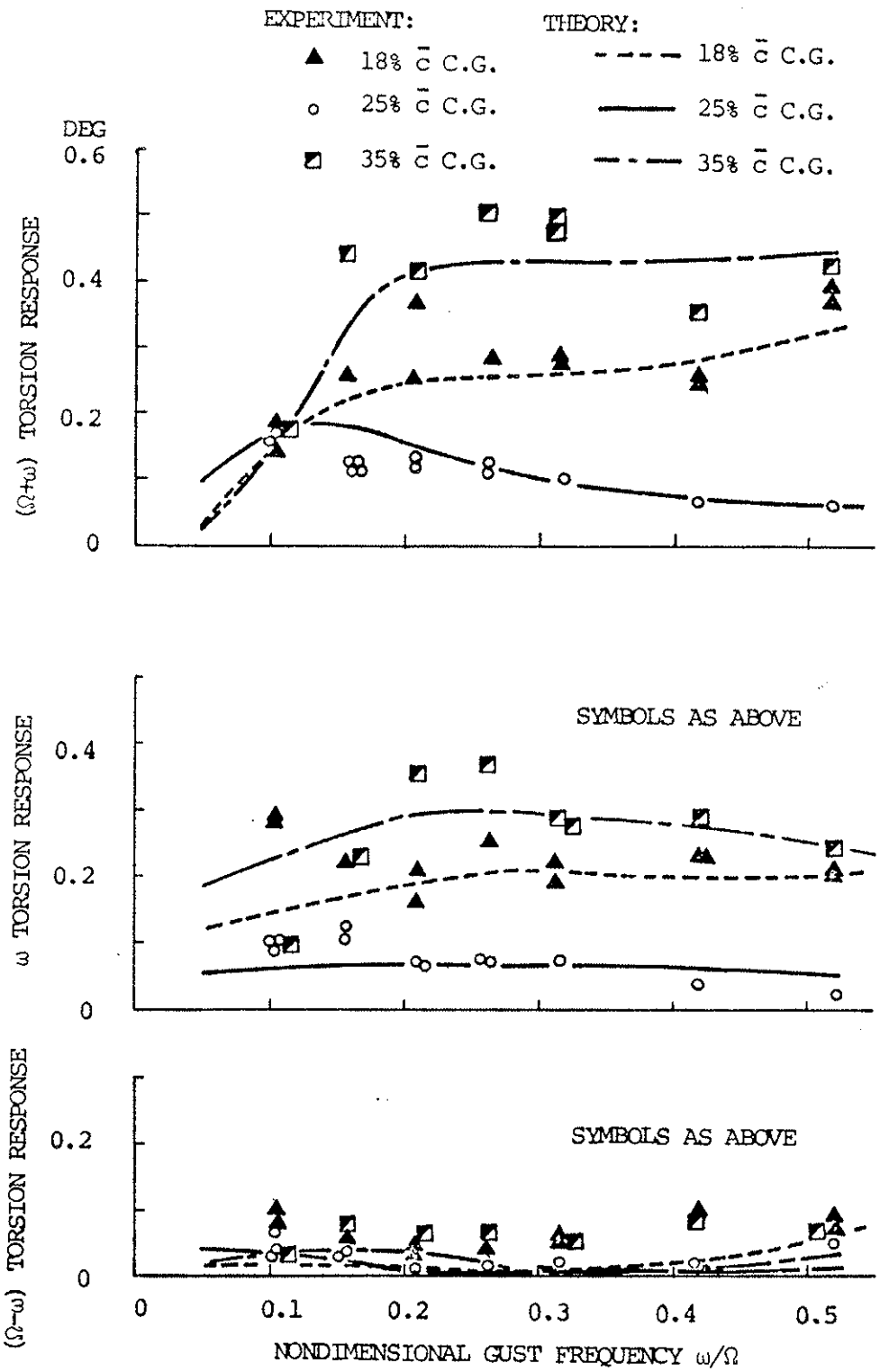

(d) TORSION RESPONSE OF "SOFT TORSION" BLADE: ω_ϕ/Ω=2.38/rev

FIG. 11 CONTINUED

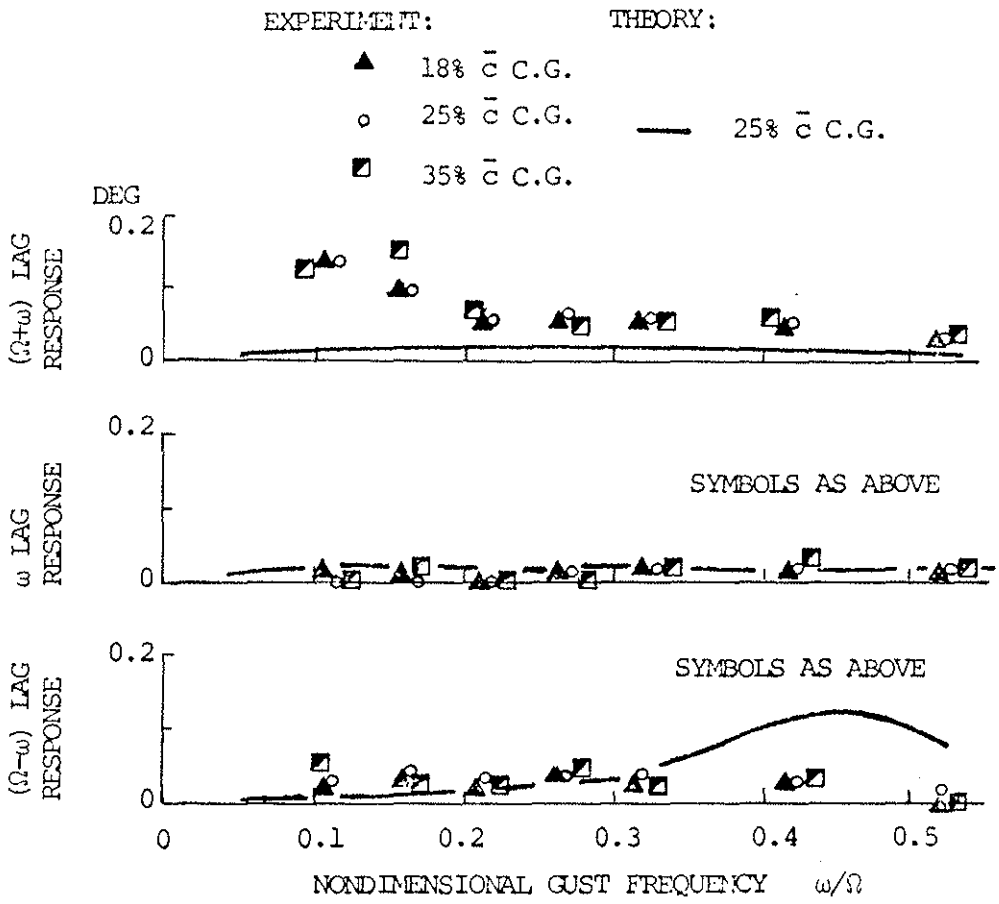

(e) LAG RESPONSE OF "STIFF TORSION" BLADE: ω_ϕ/Ω=5.21/rev

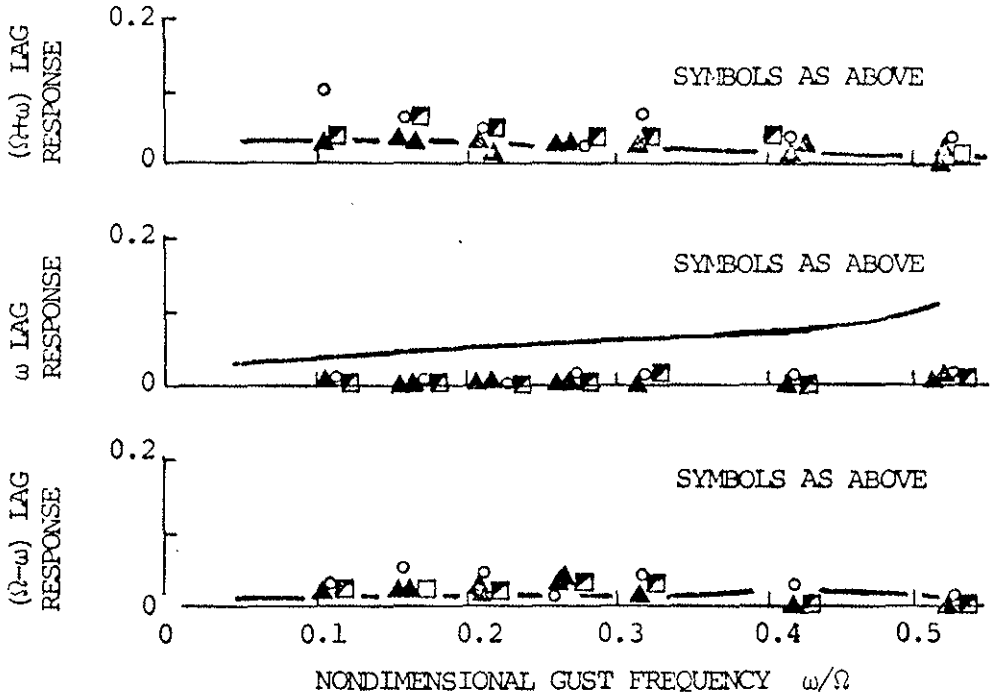

(f) LAG RESPONSE OF "SOFT TORSION" BLADE: ω_ϕ/Ω=2.38/rev

FIG. 11 CONTINUED

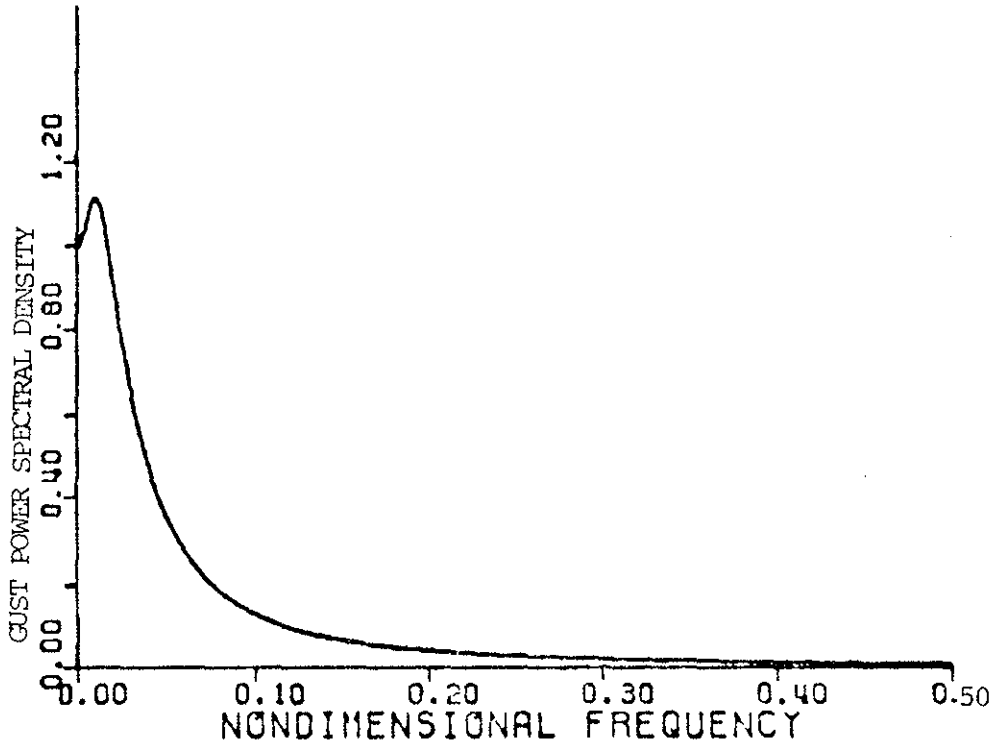

FIG. 12 VON KARMAN GUST POWER SPECTRAL DENSITY SCALED TO WIND WIND TUNNEL MODEL BLADE

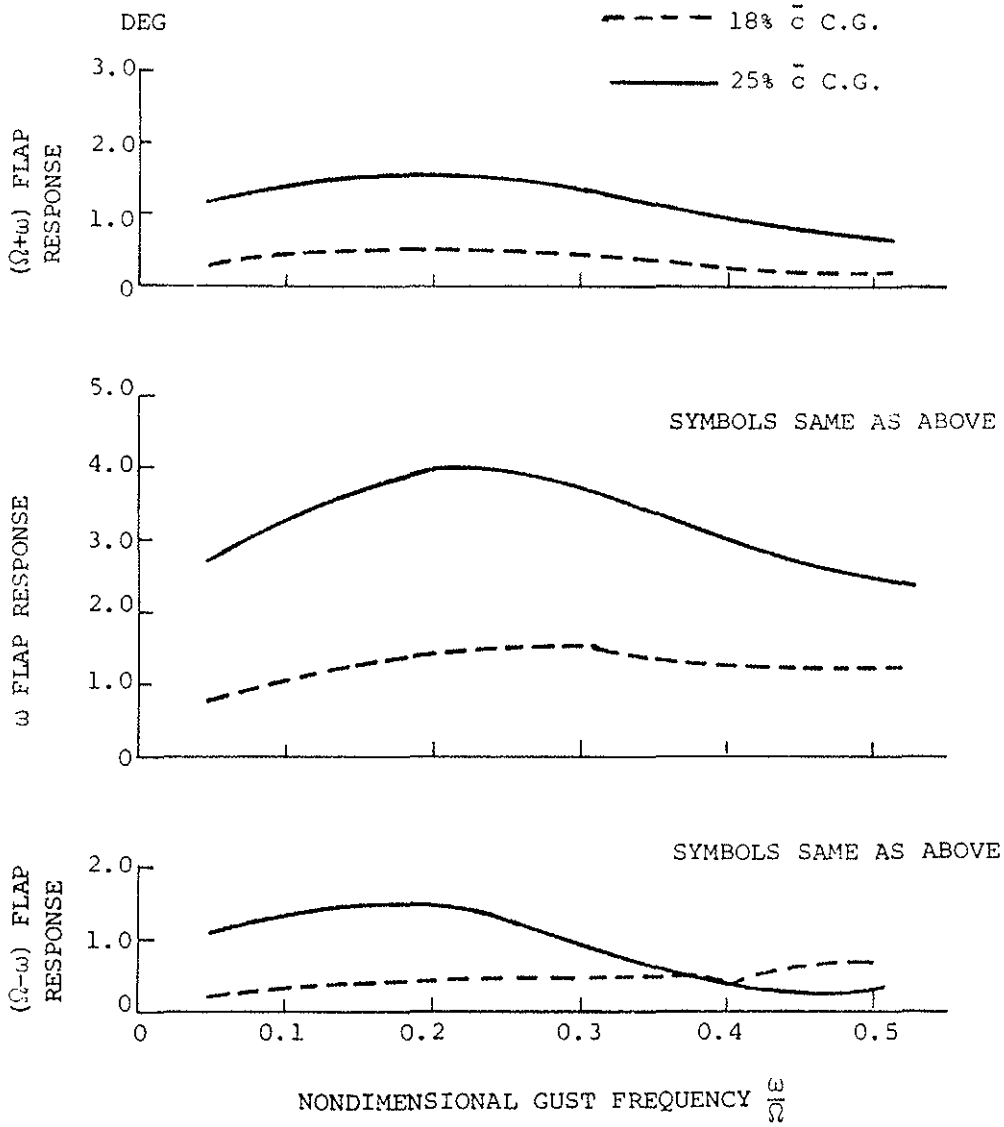

(a) Flap Response

FIG. 13 VERTICAL GUST RESPONSE OF HINGELESS ROTOR WITH LOCK NUMBER OF 10; $(\omega_\phi/\Omega) = 2.32$

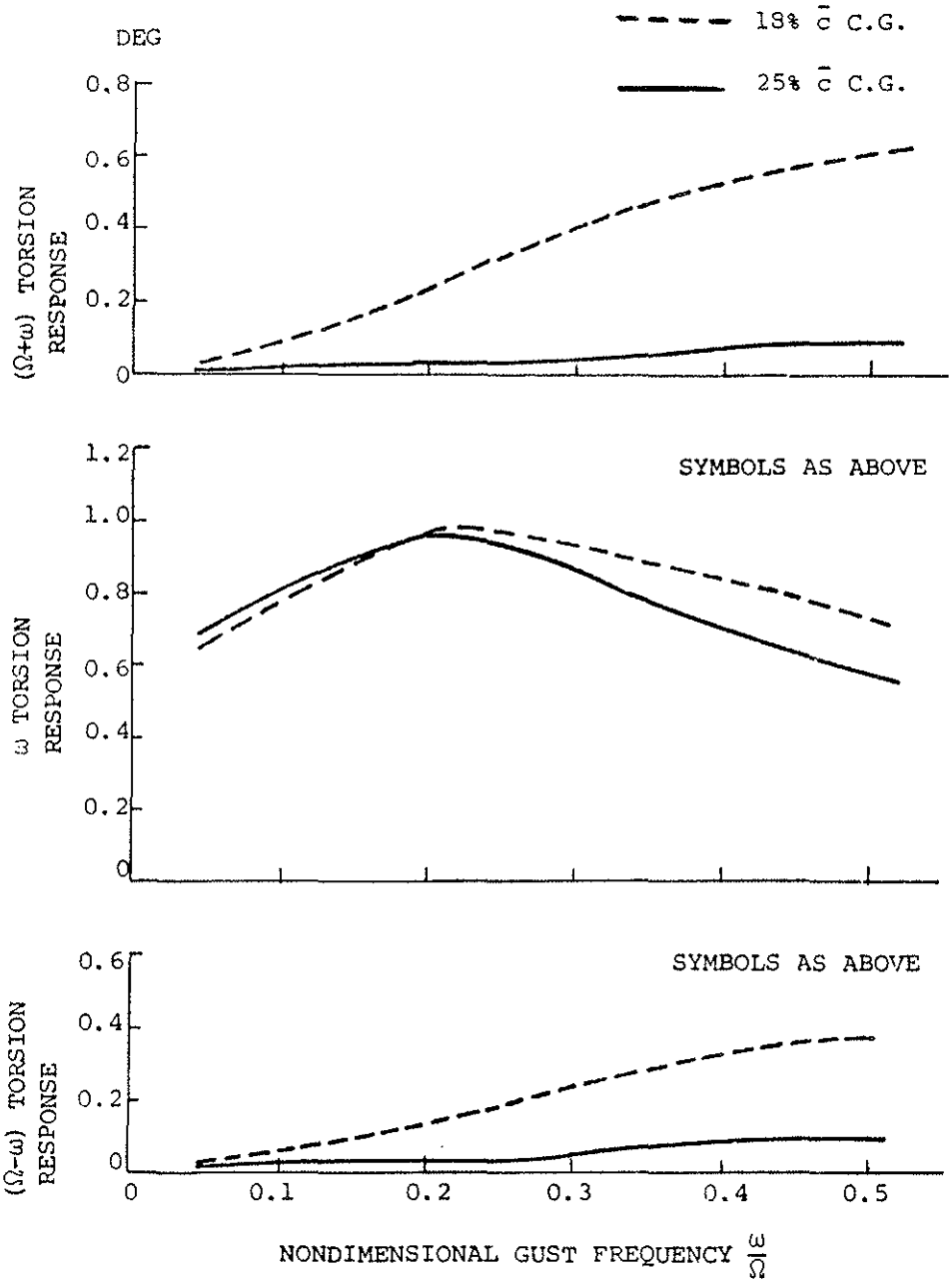

(b) Torsional Response

FIG. 13 CONCLUDED

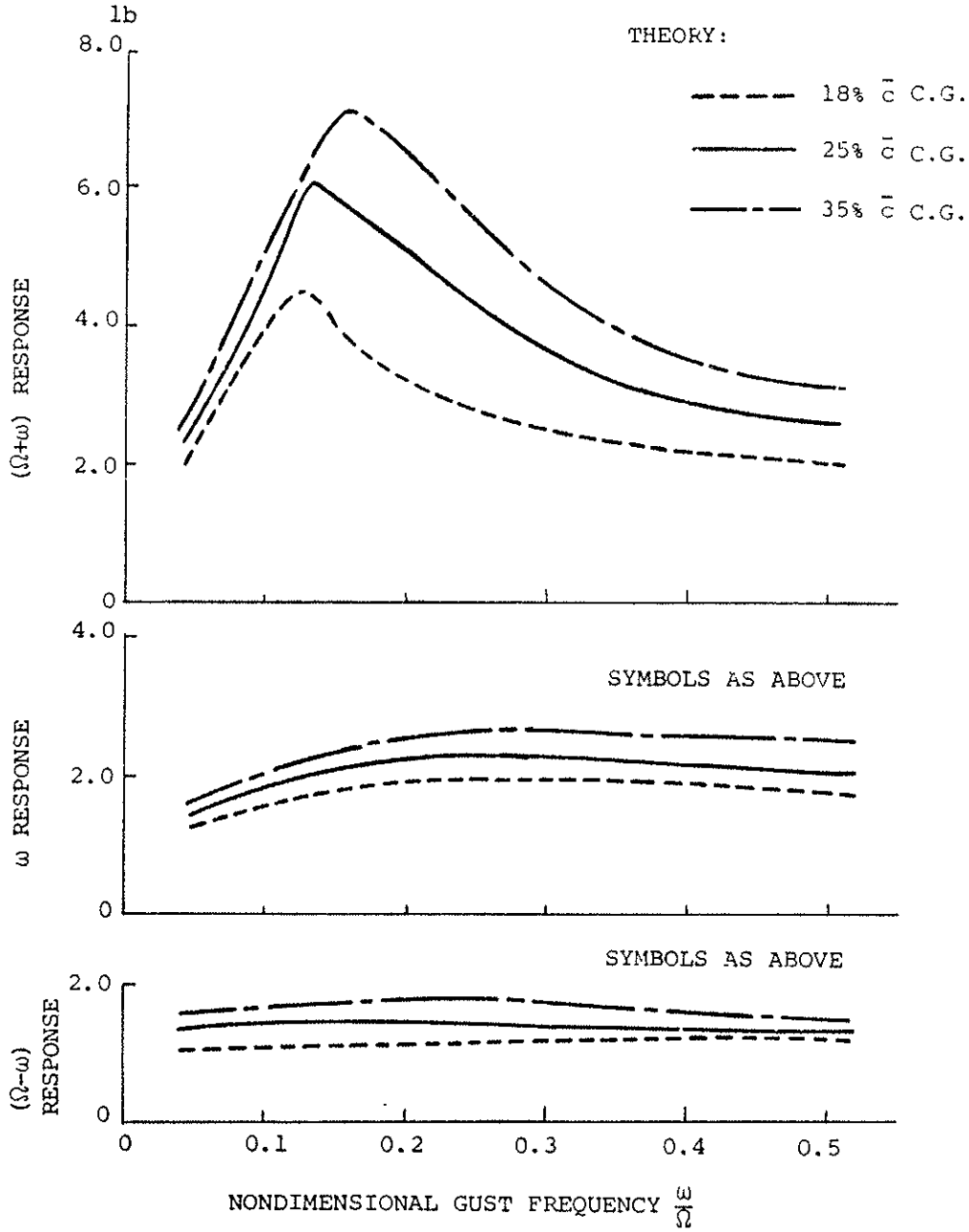

FIG. 14 VERTICAL SHEAR FORCE RESPONSE OF THE SINGLE-BLADED ROTOR TO THE VERTICAL GUST IN ADVANCE RATIO 0.384: "SOFT TORSION" BLADE $(\frac{\omega_\phi}{\Omega})$ = 2.38/REV WITH CHORDWISE C.G. SHIFT